

INTERNATIONAL ATOMIC ENERGY AGENCY

**INDC(CCP)-425**

Distr.: EL

---

**I N D C      INTERNATIONAL NUCLEAR DATA COMMITTEE**

---

**ANALYSIS AND REEVALUATION  
OF THE NEUTRON CROSS SECTIONS FOR  $^{23}\text{Na}$**

E.L. Trykov and I.R. Svinin

Institute of Physics and Power Engineering  
State Scientific Center of the Russian Federation  
1 Bondarenko sq., Obninsk, Kaluga Region, Russia 249020

Fax: +7-095-2302326  
E-mail: [trykov@ippe.rssi.ru](mailto:trykov@ippe.rssi.ru)

May 2000

Printed by the IAEA in Austria  
May 2000

## **ANALYSIS AND REEVALUATION OF THE NEUTRON CROSS SECTIONS FOR $^{23}\text{Na}$**

E.L. Trykov and I.R. Svinin

Institute of Physics and Power Engineering  
State Scientific Center of the Russian Federation  
1 Bondarenko sq., Obninsk, Kaluga Region, Russia 249020

Fax: +7-095-2302326  
E-mail: trykov@ippe.rssi.ru

### **Abstract**

The reaction model calculations of the cross sections of neutron-induced reactions on  $^{23}\text{Na}$  have been carried out for incident energies up to 20 MeV. The results of the calculations are compared to all available experimental data, including the most recent ones, and also to the previous evaluations. The discrepancies between the data and the present evaluation and also between evaluations themselves were analyzed. The probable reasons of these discrepancies were considered. On the whole, the calculation results agree well enough with the experimental data.

May 2000

## 1. Introduction

As Sodium is known to be a coolant material for fast reactors, the cross sections for neutron-induced reactions on it are of great importance. However the experimental data for some cross sections are scarce (for a example,  $(n,n')$  cross section data are not available above incident neutron energy of 5 MeV), and for other cross sections the data are in conflict with each other (for example, the  $(n,2n)$  cross section data). In such a situation it is necessary to use in evaluation the reaction model calculations because they give a possibility to interpolate and extrapolate cross sections to energy regions where no data exist, and to predict reaction cross sections for which there are few or no experimental data. In order to ensure internal consistency, the model calculations should simultaneously reproduce as much as possible the experimental information for reaction channels where reliable data are available.

The work presents the results of consistent description of cross sections for neutron induced reactions on  $^{23}\text{Na}$  obtained in the framework of the coupled channel optical model and Hauser-Feshbach statistical model with account of pre-equilibrium corrections in the formulation of exciton model. The cross sections included into consideration are total, elastic, inelastic, capture,  $(n,p)$ ,  $(n,d)$ ,  $(n,t)$ ,  $(n,\alpha)$ ,  $(n,2n)$ ,  $(n,np)$ , and  $(n,n\alpha)$  cross sections. The photon production data include multiplicities, transition probabilities and gamma-ray production cross sections and spectra. Besides, the neutron emission spectra are considered. Much effort is put into the consistency between the model calculations and the experimental data, including the most recent ones. The comparison of the present evaluation results and those of ENDF/B-VI [85] and JENDL-3.2 [86] is carried out. The evaluation is performed in the incident neutron energy range from 100 keV to 20 MeV.

## 2. Computational methods and procedures

The primary code used in the present evaluation work was GNASH [1]. It computes simultaneously the cross sections for all energetically possible single step and sequential decay binary reactions, the resulting gamma-ray production cross sections and outgoing photon and particle spectra. The resulting cross section sets are consistent and energy balance is ensured. The following improvements were made in the GNASH:

- 1) As it is known, in the low energy region the width fluctuation corrections to the average compound nucleus cross section are important, especially for calculation of the inelastic scattering cross section with excitation of the first few levels. Therefore the module for width fluctuation correction calculations using the approximate method of Tepel *et al.* [2] in the form given by Hofmann *et al.* [3] was introduced in the code.
- 2) When the closed form of the exciton model is used in the GNASH code for the pre-equilibrium contribution calculations, the internal transition rates with decreased exciton number (i.e.  $\lambda^-$ ) are neglected. As present calculations have shown, this approximation led to the sizable unphysical fluctuations of cross sections. Therefore,  $\lambda^-$  term was introduced in the preequilibrium formulae which were used in the GNASH code.

- 3) The GNASH code allows to get a simple estimate of the direct-semidirect capture spectrum within the framework of the exciton model. To achieve a better agreement with the experimental data on capture cross section we introduced in the GNASH the adjusting factor, which allowed to change the direct-semidirect contribution value.

With these modifications the GNASH code can be used in wide energy range of incident neutrons. Transmission coefficients for the GNASH were obtained by using the ECIS code [4]. The ECIS also provided the direct reaction contribution to the level excitation cross sections and some angular distributions. Parameters required as input to the GNASH and to the ECIS are discussed in Section 3.

### **3. Parameter determination**

#### *3.1. Optical-model parameters*

The differential elastic cross sections at 7.6 and 8.52 MeV [5] and the combined differential cross sections for elastic and inelastic scattering to the 0.44 MeV level at incident energies of 8.0, 9.7 [6], 14.1 [6,7] and 14.76 MeV [8] were used in an attempt to generate a consistent set of neutron optical model parameters. The search using the ECIS code was performed with the aim of fitting each angular distribution, the energy averaged total cross section and the available nonelastic cross section. In the coupled channel calculations,  $^{23}\text{Na}$  was treated in the rotational model, coupling the ground state ( $3/2^+$ ) and the excited states at 0.44 MeV ( $5/2^+$ ) and 2.08 MeV ( $7/2^+$ ). The deformation parameters were  $\beta_2 = 0.36$  and  $\beta_4 = 0.20$  as in the work of Strohmaier [9], using information from the work of Mannion *et al.* [10]. For the determination of the other parameters, no automatic search was used, but certain starting values were taken from the Ref. [9]. For the levels included in the coupling scheme the direct-interaction component of the inelastic scattering cross sections were calculated.

Compound elastic angular distribution was taken from the ECIS code but it was normalized on the value obtained from the GNASH code in a consistent way with the same transmission coefficients. It was done because it was impossible to take into account the competition between the  $(n,n')$ ,  $(n,p)$  and  $(n,\alpha)$  in the ECIS. A series of searches resulted in set of coupled channels optical model parameters which provided a good overall fit to the angular distributions as well as to the average total and nonelastic cross sections. This final set of parameters is given in Table I and the quality of the fit can be seen in Figures 1 through 6.

Proton, deuteron, triton and alpha optical-model parameters are also required for the Hauser-Feshbach analysis. The proton, deuteron and triton optical potential parameters were taken from the work of Perey and Perey [11]. The alpha optical potential parameters were taken from the work of Lemos [12]. All these parameters are given in Table I.

#### *3.2. Discrete energy levels and level-density parameters*

The statistical-model calculations with GNASH require a complete description of the levels of the residual nuclei for the various open channels. The low-energy excitation region of these nuclei can be adequately described in terms of discrete levels for which we usually

know the energy, spin and parity ( $J^\pi$ ), and gamma-ray de-excitation branching ratios. As the excitation energy increases, the information about these levels becomes incomplete, and it is preferred to describe them in terms of a level density formula.

The reactions for which we need information about the levels in residual nuclei are:  $^{23}\text{Na}(n,n')^{23}\text{Na}$ ,  $^{23}\text{Na}(n,p)^{23}\text{Ne}$ ,  $^{23}\text{Na}(n,d)^{22}\text{Ne}$ ,  $^{23}\text{Na}(n,t)^{21}\text{Ne}$ ,  $^{23}\text{Na}(n,\alpha)^{20}\text{F}$ ,  $^{23}\text{Na}(n,2n)^{22}\text{Na}$ ,  $^{23}\text{Na}(n,np)^{22}\text{Ne}$ ,  $^{23}\text{Na}(n,nd)^{21}\text{Ne}$ ,  $^{23}\text{Na}(n,n\alpha)^{19}\text{F}$ ,  $^{23}\text{Na}(n,2np)^{21}\text{Ne}$ , and  $^{23}\text{Na}(n,\gamma)^{24}\text{Na}$ . The energy of levels,  $J^\pi$  and gamma-ray branching ratios adopted for the nuclei are given in Tables from II to IX (the characteristics of the levels were taken from the compilations [87, 88]).

To represent the continuum excitation energy region laying above the highest discrete level, the Gilbert-Cameron level density formulae [13] were used. Nuclear temperature T and normalization factor  $E_0$  were taken from the RIPL [14]. For  $N, Z \leq 10$ , Gilbert and Cameron did not give the pairing energies and we used in these cases  $\Delta = 0$  for odd-odd nuclei,  $\Delta = 11 \text{ A}^{-1/2}$  for odd nuclei, and  $\Delta = 22 \text{ A}^{-1/2}$  for even-even nuclei. After that the parameter "a" was selected so that the constant temperature and the Fermi-gas functions were conjugated smoothly. Simultaneously this condition determined the boundary between two level-density regions ( $E_{\text{match}}$ ). All these parameters values were considered as initial ones and varied slightly in order to achieve the best agreement with experimental data on  $^{23}\text{Na}$ . The final values are given in the Table X. The spin-cutoff parameter  $\sigma^2$  for the discrete level region was determined by the GNASH code from discrete level data.

### 3.3. Gamma-ray strength functions

Three values of gamma-ray multipolarity, namely E1, M1 and E2, were taken into consideration. The E1 gamma-ray strength function was obtained from the expression:

$$f_{E1} = K \frac{\sigma_0 \epsilon_\gamma \Gamma^2}{(\epsilon_\gamma^2 - E^2)^2 + \epsilon_\gamma^2 \Gamma^2}, \quad (1)$$

where the peak cross section of the giant dipole resonance,  $\sigma_0$ , the width of the resonance,  $\Gamma$ , and the energy of resonance peak, E, were equal to 10 mb, 7 MeV and 20 MeV, respectively. However, in the gamma-ray energy range from 11 to 14 MeV the  $f_{E1}$  value was reduced by 70% in order to describe the experimental capture cross section shape more precisely.

The M1 gamma-ray strength function was also given by the Eq. (1), but the parameters were  $\sigma_0 = 1 \text{ mb}$ ,  $\Gamma = 4 \text{ MeV}$  and  $E = 41 \text{ A}^{-1/3} (\text{MeV})$ . A Weisskopf form, i.e. constant, was used for the E2 gamma-ray strength function. This constant and also the constant K values were equal at first to those recommended by the GNASH code in order to establish the relative contributions of E1, M1, E2 components, and then they were renormalized by means of one overall normalization to the s-wave neutron gamma-ray strength function value. This value was chosen to be  $3.9 \cdot 10^{-5}$  to describe the capture cross section data in the best way.

#### **4. The total, nonelastic and elastic cross sections**

The evaluation for the total cross section is based on coupled channel calculations with the optical-model parameters from Table I. The result of calculations is displayed in Fig. 1 together with the evaluated cross section from ENDF/B-VI based on Larson *et al.* experimental data [15]. To avoid the overloading of the figure by a huge number of experimental points these data are shown only for high energies. On the average the calculated cross section agrees rather well with the data.

In the same figure the nonelastic cross section from GNASH calculation is presented together with the ENDF/B-VI nonelastic cross section and the available experimental data which are very scarce. It is seen that in the energy range from 10 to 17 MeV the calculated cross section is smaller than ENDF/B-VI evaluation by a few tens millibarns. Accordingly the calculated elastic cross section exceeds the ENDF/B-VI evaluated elastic cross section in this region. A similar exceeding can also be seen in Fig. 5 where the sum of differential elastic and inelastic cross sections to the 0.44 MeV level of  $^{23}\text{Na}$  at 14.1 MeV incident neutron energy is shown. Because the  $^{23}\text{Na}$  ( $n, n'$ ) cross section for exciting of this level (Fig. 8) from calculation and ENDF/B-VI are practically equal at this energy, the difference is connected just with the elastic scattering.

Figures 2 through 6 show experimental angular distributions for elastic cross section or sum of elastic and first level excitation cross sections when experiment does not allow to separate them, and their description in consistent GNASH and ECIS calculations. The quality of description is rather good.

The dependence of calculated elastic scattering cross section on the incident neutron energy is shown in Fig. 7 in comparison with the available experimental data. Unfortunately, there are no data in the energy range from 10 to 17 MeV discussed above. On the average the agreement is quite good.

#### **5. The ( $n$ , particle) reactions**

All level excitation functions were calculated with the GNASH code with taking into account the direct part from the ECIS calculations with the optical parameters described above. The excitation functions for the first three levels of  $^{23}\text{Na}$  are displayed in Figures 8-10 in comparison with the experimental data and the evaluations from ENDF/B-VI and JENDL-3.2. There is a strong resonance structure in experimental data below 4-5 MeV, but at more higher incident neutron energies (to 8.5 MeV) there is an acceptable agreement between the calculated and measured data. There are no available data for the energies exceeding 8.5 MeV, and just in this region where the direct reaction mechanism gives the main contribution, the considerable differences between evaluations presented in Figures 8-10 are seen. It should be mentioned here that we used the coupled channels method, and the DWBA was used in the JENDL-3.2 evaluation.

The total inelastic cross section is shown in Fig. 11. Unfortunately there are no available experimental data for incident neutron energy above 5 MeV where big discrepancy exists between different evaluations.

There is more experimental information on the (n,p) and (n, $\alpha$ ) reactions cross sections from the thresholds to 20 MeV, and therefore much effort was put into generating a consistent evaluation of these cross sections. The comparison of the GNASH calculation results and the experimental data is shown in Fig. 12 for the (n,p) reaction and in Fig. 13 for the (n, $\alpha$ ) reaction. It is seen that these data are described by the calculation fairly good both at the low and at the high incident neutron energies. At the same time, there is the big difference between the present evaluation and the ENDF/B-VI and JENDL-3.2 evaluations for (n, $\alpha$ ) cross section in the energy range from 10.5 to 14 MeV.

There are only two available experimental points for the (n,t) reaction cross section that are presented in Fig. 14 together with the GNASH calculation results. The excellent agreement between them was achieved without any special adjustment.

As for  $^{23}\text{Na}$  (n,d) reaction cross section, it is difficult to separate  $^{23}\text{Na}$  (n,np) and  $^{23}\text{Na}$  (n,d) reactions in an experiment. Besides, the data themselves on these reactions are very scarce. The integral production of protons and deuterons with the energies exceeding 1 MeV from the reaction system  $^{23}\text{Na}$  + neutron was obtained by Aldefeld [54]. It is shown in Fig. 15 in comparison with the GNASH calculation results. The agreement is quite good. The total production of  $^{22}\text{Ne}$  at 14.5 MeV measured by Leich *et al.* [51] and the corresponding calculated result are in less agreement: the experimental value is  $330 \pm 17$  mb, and the calculated value is 298 mb.

A certain information on the (n,np) and (n,pn) reactions was obtained by Aldefeld [54] from the integrated proton single spectrum and from proton spectra measured in coincidence with neutrons. The proton production from these reactions (outgoing particle energy > 1 MeV) is shown in Fig. 16 in comparison with the GNASH calculation results. The sizable discrepancy exists between two sets of experimental points, and the calculated cross section agrees with one of them rather well. Besides, the  $^{23}\text{Na}[(\text{n,np})+(\text{n,pn})]$  cross section at the incident neutron energy of 14.6 MeV was obtained by Kozyr *et al.* [68]. It is equal to  $300 \pm 50$  mb, and the calculated value is 269 mb.

The most investigated from two particle emission reactions is the  $^{23}\text{Na}(\text{n},2\text{n})^{22}\text{Na}$  reaction. There are two groups of experimental cross sections which differ by a factor of about 2. Therefore special studies, for example the work of Strohmaier [9] and of Strohmaier *et al.* [59], were devoted to the solution of this problem. In consent with the works [9,59], the present evaluation leans on the lower-lying experimental results. The calculated (n,2n) reaction cross section is displayed in Fig. 17 together with the available experimental data. It agrees with the most recent data of Filatenkov *et al.* [65], Lu *et al.* [58], Sacuma *et al.* [66] and Strohmaier *et al.* [59] very well.

For the testing of the calculated (n,n $\alpha$ ) and (n, $\alpha$ n) reactions cross sections the experimental data on  $\alpha$ -particle production from the reaction system  $^{23}\text{Na}$  + neutron were used. These data and the calculation results are presented in Fig. 13. They agree with each other rather well.

## 6. Neutron emission spectra

Neutron emission spectra were calculated with the GNASH for all incident neutron energies. However, the measurements exist only for the energies of 14.1 and 14.6 MeV [7, 69, 70]. The comparison of calculated spectrum at 14.1 MeV with the experimental data of Priller *et al.* [7] is shown in Figure 18. At energy about 6.3 MeV, the measured spectrum displays a maximum which is reproduced by the present calculation rather well due to extension of discrete level scheme up to 7.87 MeV on excitation energy (48 levels, see Table III). Such possibility to reduce the discrepancy between the measured and calculated spectra in this region was discussed in Ref. [7].

The attempt was also done in the present calculation to improve the agreement with the measured spectrum around 3 MeV by the embedding a few discrete levels in the continuum of  $^{23}\text{Na}$  levels at the excitation energy from 9.8 to 10.7 MeV (levels from 49 to 65 in Table III). A certain improvement was achieved by this way. So a quite good agreement at the energy of secondary neutrons near 6.3 and 3.0 MeV is accounted by the local fluctuations of the level density at appropriate excitation energies. It is the only way for the simultaneous description of the neutron production spectra and  $^{23}\text{Na}(n,2n)^{22}\text{Na}$  reaction cross section. If someone would try to reproduce the neutron emission spectra shape by increasing of smooth part of the level density itself he immediately got the reduction of total inelastic cross section and increasing of  $(n,2n)$  cross section.

In Fig. 19 the comparison between the measured and the calculated neutron production spectra at 14.6 MeV incident neutron energy is shown. It should be emphasized that the data of Takahashi *et al.* [70] are given at 5 angles in the laboratory system. Therefore the angle integration and transformation to the center-of-mass system were approximated in a crude manner in the work of Strohmaier [9] and its results were used in present work for comparison with the appropriate calculation and with the data of Hermsdorf *et al.* [69]. The uncertainties of the Hermsdorf *et al.* data were increased two times with respect to [69], as it was recommended by Strohmaier [9]. The calculation agrees reasonably well with the measurements.

## 7. Capture and gamma-ray production cross sections

The experimental data on the neutron capture cross section, especially the data of Menlove *et al.* [32], were used for the choice of the gamma-ray strength function parameters (see Section 3.3). It is not surprising therefore that the calculated capture cross section agrees with the measured data fairly well, as it is seen from Fig. 20. It should be mentioned that the adjusting factor for the direct-semidirect contribution discussed in Section 2 was equal to 1.8 in the present calculation.

As discussed above, the consistent reaction model analysis allowed to reproduce the available data from  $(n, \text{ particle})$  and  $(n,\gamma)$  reactions reasonably well. The results of this analysis and gamma-ray branching ratios (see Tables II-IX) were used to calculate the gamma-ray production cross sections for these reactions. The calculated excitation functions for production of five gamma rays in  $^{23}\text{Na}$  are shown in Figures 21-26 in comparison with available experimental data. The experimental data for most representative  $(n,\alpha\gamma)$  reaction cross sections are compared with the results of calculations in Figures 27 and 28. In general,

the results of calculations are a good compromise for evaluation in case of discrepant experimental data.

The calculated gamma-ray production spectra are compared to the data measured by Larson *et al.* [83] in Figures 29 through 31. Calculations were done in a few points of incident neutron energy region for which average experimental values of [83] were given. Then all calculated spectra were averaged with the weight of incident neutron spectra taken from the work of Dickens *et al.* [84]. Although the measurement, as well as the GNASH calculations, were made at many incident neutron energies, comparison are shown only for energy intervals: 9.98 - 12.03, 12.03 - 14.02, and 14.02 - 17.04 MeV. In general, the calculations reproduce well the experimental data, and provide additional information on the cross sections for  $E_\gamma < 0.5$  MeV. Recent data of Nefedov *et al.* [89] at incident neutron energy 14.3 MeV are shown in Figure 32 in comparison with the result of present calculation and the agreement is good too.

As it is shown in Figure 33 the total gamma production cross section is also in a quite good agreement with the previous evaluations [85, 86].

## 8. Summary and conclusions

Advanced nuclear model codes and recently improved experimental data were used for evaluation of  $^{23}\text{Na}$  neutron cross sections. Cross sections for all important reactions, with pre-equilibrium effects included, are given. Neutron, charged particles and gamma-ray spectra are presented. The present  $^{23}\text{Na}$  evaluation, based on model calculations for incident neutron energies above the region with resonance structures in cross sections, is improved over previous ones [85, 86] and can be recommended for practical use. It is especially true for  $(n,2n)$  reaction for which the new experimental data were obtained recently. In present calculation all possible decay channels for incident neutron energies under consideration were taken into account and though there are still no measured data for total inelastic cross section above 5 MeV, it is possible to suppose that the calculated total inelastic cross section differs from the true one not too much. This work results will be used for the creation of  $^{23}\text{Na}$  evaluated file of BROND-3 library.

The authors are grateful to A.V. Ignatyuk and V.P. Lunev for very helpful discussions. Partial support of this work by the ISTC-731-97 project is gratefully acknowledged.

## REFERENCES

- [1] YOUNG, P.G., ARTHUR, E.D., Los Alamos National Laboratory Report LA-6947 (1977) 153.
- [2] TEPEL, J.W., HOFMANN, H.M., WEIDENMUELLER, H.A., Phys. Lett. **B49** (1974) 1.
- [3] HOFMANN, H.M., MERTELMEIER T., HERMAN, M., TEPEL, J.W., Z. Physik **A297** (1980) 153.
- [4] RAYNAL, J., International Atomic Energy Agency Report IAEA SMR-9/8 (1970) 281.
- [5] PEREY, F.G., KINNEY, W.G., Report ORNL/TM-4518, Oak Ridge National Lab., TN (1970).

- [6] FASOLI, U., et al., Report CEC(73)-7, Univ. of Padua (1973).
- [7] PRILLER, A., et al., Phys. Rev. **C56** (1997) 1424.
- [8] KUIJPER, P., VEEFKIND, J.C., JONKER, C.C., Nucl. Phys. **A181** (1972) 545.
- [9] STROHMAIER, B., Ann. Nucl. Energy **20** (1993) 533.
- [10] MANNION, M.C., et al., J. Phys. G: Nucl. Phys. **14** (1988) 1093.
- [11] PEREY, C.M., PEREY, F.G., Atomic Data and Nuclear Data Table **13** (1974) 293.
- [12] LEMOS, O.F., Orsey, Series A, No. 136 (1972).
- [13] GILBERT, A., CAMERON, A.G.W., Can. J. Phys. **43** (1965) 1446.
- [14] BELGYA, T., et al., INDC(NDS)-367 (1997).
- [15] LARSON, D.C., HARVEY, J.A., HILL, N.W., Report ORNL-TM-5614 (1976).
- [16] POZE, K.R., GLAZKOV, N.P., Sov. Phys. - JETP **3** (1956) 745.
- [17] STRIZHAK, V.I., Sov. Phys. - JETP **4** (1957) 769.
- [18] PEREY, F.G., KINNEY, W.E., Report ORNL-4518 (1970).
- [19] KINNEY, W.E., McCONNELL, J.W., Proc. of the Int. Conf. on Interactions of Neutrons with Nuclei, Lowell **2** (1976) 1319.
- [20] CHIEN, J.P., SMITH, A.B., Nucl. Sci. Eng. **26** (1966) 500.
- [21] COLES, R.E., Report AWRE-0-03/71 (1971).
- [22] FASOLI, U., et al., Nucl. Phys. **A125** (1969) 227.
- [23] TOWLE, J.H., GILBOY, W.B., Nucl. Phys. **32** (1962) 610.
- [24] SCHWEITZER, TH., SEELIGER, D., UNHOLZER, S., Proc. of the Fourth All Union Conf. on Neutron Physics, Kiev, 1977, **1** (1977) 231.
- [25] TOWLE, J.H., OWENS, R.O., Nucl. Phys. **A100** (1967) 257.
- [26] SHIPLEY, E.N., OWEN, G.E., MADANSKY, L., Phys. Rev. (1959) 115, 122.
- [27] DONATI, D.R., et al., Phys. Rev. **C16** (1977) 939.
- [28] SIGG, R.A., Dissertation Abstracts **B37** (1976) 2237.
- [29] MACKLIN, R.L., GIBBONS, J.H., INADA, T., Phys. Rev. **129** (1963) 2695.
- [30] MACKLIN, R.L., LAZAR, N.H., LYON, W.S., Phys. Rev. **107** (1957) 504.
- [31] BAME, S.J., Jr., CUBITT, R.L., Phys. Rev. **113** (1959) 256.
- [32] MENLOVE, H.O., et al., Phys. Rev. **163** (1967) 1299.
- [33] MAGNUSSON, G., ANDERSSON, P., BERQUIST, I., Physica Scripta **21** (1) (1980) 21.
- [34] PERKIN, J.L., O'CONNOR, L.P., COLEMAN, R.F., Proc. Phys. Soc. **72** (1958) 505.
- [35] CSIKAI, J., et al., Nucl. Phys. **A95** (1967) 229.
- [36] LYON, W.S., MACKLIN, R.L., Phys. Rev. **114** (1959) 1619.
- [37] HOLUB, E., et al., Report LNS-4-72 (1972).
- [38] PEREY, F.G., KINNEY, W.E., MACKLIN, R.L., Proc. of the Third Conference on Neutron Cross Sections and Technology, Univ. of TN, Knoxville (1971) 191.
- [39] PAUL, E.B., CLARKE, R.L., Can. J. Phys. **31** (1953) 167.
- [40] ALLAN, D.L., Nucl. Phys. **24** (1961) 274.
- [41] CSIKAI, J., NAGY, S., Nucl. Phys. **A91** (1967) 222.
- [42] MUKHERJEE, S.K., GANGULY, A.K., MAJUMDER, M.K., Proc. Phys. Soc. (Lond.) **77** (1961) 508.
- [43] KHURANA, C.S., GOVIL, I.M., Nucl. Phys. **69** (1965) 153.
- [44] JANCZYSZYN, J., Proc. Int. Conf. on Nuclear Data for Science and Technology, Antwerp, 1982, (1983) p. 869.
- [45] SCHANTL, W., Thesis, Univ. of Vienna (1970).
- [46] BARTLE, C.M., Nucl. Instrum. Methods in Phys. Res. **124** (1975) 547.
- [47] WILLIAMSON, C.F., Phys. Rev. **122** (1961) 1877.

- [48] WEIGMANN, H., et al., Proc. Int. Conf. on Nuclear Data for Science and Technology, Antwerp, 1982, (1983) p. 814.
- [49] PICARD, J., WILLIAMSON, C.F., Nucl. Phys. **63** (1965) 673.
- [50] QAIM, S.M., WOELFLE, R., Nucl. Phys. **A295** (1978) 150.
- [51] LEICH, D.A., BORG, R.J., LANIER, V.B., Paper presented at the 16<sup>th</sup> Lunar and Planetary Conf., Houston, TX (1985); and EXFOR 12918.
- [52] WOELFER, G., BORMANN, M., Z. Phys. **194** (1966) 75.
- [53] PEPELNIK, R., et al., Report NEANDC(E)-262U (1985) p. 32.
- [54] ALDEFELD, B., Nucl. Phys. **A145** (1970) 569.
- [55] NGOC, P.N., et al., Report ZfK-410 (1980) p. 192.
- [56] STRAIN, J.E., ROSS, W.J., Report ORNL-3672, Oak Ridge National Lab., TN (1965).
- [57] BIZETTI, P.G., BIZETTI-SONA, A.M., BICCIOLINI, M., Nucl. Phys. **36** (1962) 38.
- [58] LU, H., ZHAO, W., YU, W., Chin. J. Nucl. Phys. **14** (1992) 83.
- [59] STROHMAIER, B., WAGNER, M., VONACH, H., Proc. Int. Conf. on Nuclear Data for Science and Technology, Juelich, 1991, (1992) p. 663.
- [60] MENLOVE, H.O., et al., Phys. Rev. **163** (1967) 1308.
- [61] LISKIEN, H., PAULSEN, A., Nucl. Phys. **63** (1965) 393; and PAULSEN, A., Private communication to CCDN (1965).
- [62] IKEDA, Y., et al., Report JAERI-1312 (1988).
- [63] SHANI, G., Report INIS-MF-3663 (1976) p. 83.
- [64] ADAMSKI, L., HERMAN, H., MARCINKOWSKI, A., Ann. Nucl. Energy **7** (1980) 397.
- [65] FILATENKOV, A.A., et al., Report INDC(CCP)-402 (1997).
- [66] SAKUMA, M., et al., Paper presented at a Symp. on Nuclear Data, JAERI, Tokai (1991).
- [67] XU, et al., Proc. Int. Conf. on Nuclear Data for Science and Technology, Juelich, 1991, (1992) p. 666.
- [68] KOZYR', J.U.E., PLYUYKO, V.A., PROKOPETS, G.A., Proc. of the Fourth All Union Conf. on Neutron Physics, Kiev, 1977, **1** (1977) 276; and EXFOR 40596.
- [69] HERMSDORF, D., et al., EXFOR, File of Experimental Nuclear Reaction Data, Entry 30397.
- [70] TAKAHASHI, A., et al., OKTAVIAN Report A-87-01, Osaka Univ. (1987).
- [71] SMITH, D.L., Nucl. Sci. Eng. **64** (1977) 897.
- [72] LIND, D.A., DAY, R.B., Ann. Phys. **12** (1961) 485.
- [73] MARTIN, P.W., STEWART, D.T., J. Nucl. Energy **19** (1965) 447.
- [74] DEGTJAREV, A.P., KRAVSOV, V.V., PROCOPEC, G.A., Ukr. Fiz. Zh. **22** (1977) 1465.
- [75] SMITH, D.L., Report ANL-7710 (1971) 15.
- [76] ABBONDANNO, U., et al., J. Nucl. Energy **27** (1973) 227.
- [77] ENGESSION, F.C., THOMPSON, W.E., J. Nucl. Energy **21** (1967) 487.
- [78] TUCKER, W.E., NELLIS, D.O., MORGAN, I.L., Bull. Amer. Phys. Soc. **13** (1968) 874.
- [79] YAMAMOTO, T., et al., J. Nucl. Sci. Technol. **15** (1978) 797.
- [80] DICKENS, J.K., Nucl. Sci. Eng. **50** (1973) 98.
- [81] LACHKAR, J., PATIN, Y., SIGAUD, J., Proc. of the Second All Union Conf. on Neutron Physics, Kiev, 1973, **3** (1974) 187.
- [82] HLAVAC, S., et al., Report INDC(NDS)-357 (1996) 23.
- [83] LARSON, D.C., MORGAN, G.L., Nucl. Sci. Eng. **75** (1980) 151.
- [84] DICKENS, J.K., MORGAN, G.L., PEREY, F.G., Nucl. Sci. Eng. **50** (1973) 311.

- [85] ENDF/B-VI, Evaluated Nuclear Data File, Report BNL-NCS-17541, 4<sup>th</sup> edn (ENDF-201: ENDF/B-VI Summary Documentation) (Compiled & edited by ROSE, P.F.). National Nuclear Data Center, Brookhaven National Lab., Upton, NY (1991).
- [86] NAKAGAVA, et al., “Japanese Evaluated Nuclear Data Library, Version 3, Revision 2”, J. Nucl. Technol. **32** (1995) 1259.
- [87] ENDT, P.M., Nucl. Phys. **A521** (1990) 1. Data extracted from the ENSDF database.
- [88] AJZENBERG-SELOVE, F., Nucl. Phys. **A475** (1987) 1. Data extracted from the ENSDF database.
- [89] Yu.Ya.Nefedov *et al.*, Paper presented at the 9<sup>th</sup> Int. Conf. on Radiation Shielding, Tsukuba (1999).

**Table 1 Optical-model parameters**

Neutrons			
	$V(\text{MeV})$	$= 52.6 - 0.26E$	$r_V(\text{fm}) = 1.17$
	$W(\text{MeV})$	$= 0.045E$	$a_V(\text{fm}) = 0.65$
	$W_D(\text{MeV})$	$= 2.6 + 0.12E$	$r_W(\text{fm}) = 1.17$
	$V_{SO}(\text{MeV})$	$= 6.0$	$a_W(\text{fm}) = 0.65$
Protons			
	$V(\text{MeV})$	$= 51.0 - 0.4E$	$r_{V_D}(\text{fm}) = 1.17$
	$W(\text{MeV})$	$= 0.0$	$a_{V_D}(\text{fm}) = 0.65$
	$W_D(\text{MeV})$	$= 11.0$	$r_V(\text{fm}) = 1.25$
	$V_{SO}(\text{MeV})$	$= 7.5$	$a_W(\text{fm}) = 0.47$
	$V_{Coul}(\text{MeV})$		$a_{V_D}(\text{fm}) = 0.47$
Deuterons			
	$V(\text{MeV})$	$= 88.14 - 0.22E$	$r_V(\text{fm}) = 1.15$
	$W(\text{MeV})$	$= 0.0$	$a_V(\text{fm}) = 0.81$
	$W_D(\text{MeV})$	$= 14.4 + 0.24E$	$r_{W_D}(\text{fm}) = 1.34$
	$V_{SO}(\text{MeV})$	$= 7.0$	$a_{W_D}(\text{fm}) = 0.68$
	$V_{Coul}(\text{MeV})$		$a_{V_{SO}}(\text{fm}) = 0.5$
Tritons			
	$V(\text{MeV})$	$= 164.7 - 0.17E$	$r_V(\text{fm}) = 1.2$
	$W(\text{MeV})$	$= 40.76 - 0.33E$	$a_V(\text{fm}) = 0.89$
	$W_D(\text{MeV})$	$= 0.0$	$r_W(\text{fm}) = 1.4$
	$V_{SO}(\text{MeV})$	$= 2.5$	$a_W(\text{fm}) = 0.89$
	$V_{Coul}(\text{MeV})$		$a_{V_{SO}}(\text{fm}) = 0.72$
Alphas			
	$V(\text{MeV})$	$= 193.0 - 0.15E$	$r_V(\text{fm}) = 1.37$
	$W(\text{MeV})$	$= 0.0$	$a_V(\text{fm}) = 0.56$
	$W_D(\text{MeV})$	$= 21.0 + 0.25E$	$r_{W_D}(\text{fm}) = 1.37$
	$V_{Coul}(\text{MeV})$		$a_{W_D}(\text{fm}) = 0.56$

$E$  = incident energy (MeV),

$V$  = real well depth,

$W$  = imaginary well depth (Saxon-Woods),

$W_D$  = imaginary well depth (Saxon-Woods derivative),

$V_{SO}$  = spin-orbit potential depth,

$r_V, r_W, r_{W_D}, r_{V_{SO}}, r_{V_{Coul}}$  = radii for various potentials,

$a_V, a_W, a_{W_D}, a_{V_{SO}}$  = diffuseness for various potentials.

**Table 2** Energy levels and gamma-ray branching ratios (normalized on unity) of  $^{24}\text{Na}$ 

No.	Levels		Decays				
	E <sub>lev</sub> (MeV)	J <sup>π</sup>	Number of state (branching ratio)				
1	0	4.0					
2	0.472207	1.0	1(1.00)				
3	0.5632	2.0	1(.038)	2(.962)			
4	1.34143	2.0	2(.952)	3(.048)			
5	1.34465	3.0	1(.621)	3(.379)			
6	1.34663	1.0	2(1.00)				
7	1.5124	5.0	1(1.00)				
8	1.84601	2.0	2(.250)	3(.191)	4(.050)	5(.111)	6(.398)
9	1.88551	3.0	1(.350)	3(.650)			
10	2.51351	3.0	1(.040)	3(.960)			
11	2.5628	4.0	1(.328)	5(.521)	7(.151)		
12	2.90394	3.0	1(.118)	3(.030)	4(.493)	5(.320)	8(.039)
13	2.97783	2.0	1(.007)	2(.241)	3(.321)	4(.331)	5(.079)
14	3.2167	4.0	5(1.00)				
15	3.37184	2.0-	3(.222)	4(.299)	5(.048)	6(.410)	9(.016)
16	3.41325	1.0	2(.280)	3(.110)	4(.430)	6(.121)	9(.059)
17	3.58926	1.0	2(.230)	3(.692)	4(.028)	6(.033)	8(.017)
18	3.62825	3.0	1(.500)	4(.500)			
19	3.65597	2.0	2(.151)	3(.581)	4(.070)	8(.070)	9(.128)
20	3.68179	0.0	2(1.00)				
21	3.74509	3.0-	1(.020)	3(.109)	4(.109)	5(.211)	8(.421)
			10(.059)				9(.071)
22	3.896	2.0-	3(.222)	4(.299)	5(.048)	6(.410)	9(.016)
23	3.9357	2.0	3(.621)	4(.379)			
24	3.94339	4.0	1(1.00)				
25	3.97732	1.0-	2(.471)	3(.311)	6(.201)	8(.017)	
26	4.04849	0.0-	2(.490)	6(.510)			
27	4.145	4.0-	1(.500)	11(.500)			
28	4.1868	2.0	1(.048)	6(.262)	9(.690)		
29	4.1963	1.0-	2(.649)	3(.208)	8(.091)	13(.052)	
30	4.20719	2.0	2(.006)	3(.110)	4(.229)	6(.269)	8(.151)
			13(.023)	15(.170)	16(.032)		10(.010)
31	4.22	4.0	1(.099)	7(.901)			
32	4.44154	2.0-	2(.035)	3(.299)	4(.218)	5(.290)	8(.081)
			10(.066)	16(.004)			9(.007)
33	4.459	2.0	3(.521)	4(.479)			
34	4.526	3.0-	3(.109)	4(.109)	5(.211)	8(.441)	9(.071)
35	4.56206	1.0-	2(.351)	8(.559)	13(.040)	19(.050)	

**Table 3 Energy levels and gamma-ray branching ratios (normalized on unity) of  $^{23}\text{Na}$** 

No.	Levels		Decays			
	$E_{lev}(\text{MeV})$	$J^\pi$	Number of state (branching ratio)			
1	0.000000	1.5				
2	0.439991	2.5	1(1.00)			
3	2.076010	3.5	1(0.089)	2(0.911)		
4	2.390730	0.5	1(0.657)	2(0.343)		
5	2.639860	-0.5	1(1.00)			
6	2.703500	4.5	2(.649)	3(.351)		
7	2.982060	1.5	1(.586)	2(.411)	4(.003)	
8	3.677600	-1.5	2(.786)	4(.013)	5(.196)	7(.005)
9	3.848070	-2.5	1(.229)	2(.095)	3(.611)	5(.045)
10	3.914240	2.5	1(.795)	2(.081)	3(.090)	4(.011)
11	4.429630	0.5	1(.940)	4(.060)		
12	4.774610	3.5	2(.668)	3(.294)	6(.038)	
13	5.378560	2.5	1(.150)	2(.573)	3(.206)	7(.071)
14	5.534000	5.5	3(.210)	6(.790)		
15	5.741800	2.5	1(.753)	2(.247)		
16	5.766030	1.5	1(.511)	2(.430)	5(.044)	9(.015)
17	5.778000	1.5	1(.489)	2(.511)		
18	5.926800	3.5	1(.538)	2(.240)	3(.136)	10(.067)
19	5.964400	-1.5	1(.100)	2(.100)	4(.100)	5(.500)
20	6.042190	-3.5	2(.360)	8(.119)	9(.493)	10(.028)
21	6.115000	2.5	3(.167)	6(.833)		
22	6.194600	-2.5	1(.109)	5(.231)	8(.340)	9(.320)
23	6.236000	6.5	6(.877)	14(.123)		
24	6.307960	0.5	4(1.00)			
25	6.354500	-4.5	3(.133)	6(.179)	9(.663)	14(.025)
26	6.577790	2.5	2(.249)	3(.429)	6(.180)	10(.142)
27	6.617900	2.5	1(.038)	2(.912)	3(.011)	10(.011)
28	6.735500	1.5	2(.478)	3(.340)	8(.182)	
29	6.819600	-2.5	8(.401)	9(.599)		
30	6.867700	1.5	1(.180)	2(.820)		
31	6.920610	-1.5	1(.699)	2(.301)		
32	6.947400	1.5	1(.172)	2(.191)	4(.150)	5(.081)
33	7.070820	3.5	1(.910)	10(.090)		7(.313)
34	7.081900	-1.5	1(.552)	2(.249)	5(.199)	
35	7.122000	1.5	1(1.00)			
36	7.133200	2.5	1(.439)	2(.297)	3(.132)	7(.132)
37	7.267000	1.5	6(.529)	21(.360)	23(.111)	
38	7.277100	-2.5	3(.600)	9(.400)		
39	7.390000	1.5	6(1.00)			
40	7.412400	2.5	2(.450)	3(.310)	10(.240)	
41	7.451500	2.5	2(.900)	4(.030)	9(.070)	
42	7.487840	-1.5	4(.350)	5(.200)	8(.450)	
43	7.566200	2.5	1(.300)	2(.200)	9(.500)	
44	7.686000	1.5	5(.500)	7(.500)		
45	7.724450	0.5	1(.750)	7(.250)		
46	7.750500	2.5	2(.500)	7(.500)		
47	7.834130	2.5	2(.580)	6(.220)	10(.200)	
48	7.872830	1.5	2(.500)	4(.200)	7(.300)	
49*	9.802000	1.5	14(.199)	23(.510)	37(.291)	
50*	9.835200	1.5	2(.300)	9(.200)	16(.500)	
51*	9.849700	0.5	1(.200)	11(.300)	16(.500)	
52*	10.003000	-0.5	1(.400)	11(.300)	17(.300)	
53*	10.016400	2.5	2(.500)	9(.200)	19(.300)	
54*	10.169270	2.5	2(.500)	9(.200)	19(.300)	
55*	10.231200	2.5	2(.300)	8(.400)	19(.300)	
56*	10.338300	-0.5	1(.600)	11(.300)	17(.100)	
57*	10.345700	2.5	2(.500)	12(.200)	18(.300)	
58*	10.353400	1.5	2(.400)	13(.400)	15(.200)	
59*	10.440100	2.5	1(.150)	15(.500)	18(.350)	
60*	10.478400	1.5	2(.200)	8(.400)	15(.400)	
61*	10.501400	-1.5	1(.100)	10(.300)	13(.600)	
62*	10.507400	0.5	12(.200)	16(.500)	19(.300)	
63*	10.518600	2.5	18(.500)	20(.500)		
64*	10.548800	2.5	18(.500)	20(.500)		
65*	10.704000	-1.5	15(.500)	16(.500)		

<sup>\*</sup> Imbedded levels

**Table 4 Energy levels and gamma-ray branching ratios (normalized on unity) of  $^{22}\text{Na}$**

No.	Levels		Decays			
	E <sub>lev</sub> (MeV)	J $\pi$	Number of state (branching ratio)			
1	0	3.0				
2	0.58303	1.0	1(1.00)			
3	0.657	0.0	2(1.00)			
4	0.89089	4.0	1(1.00)			
5	1.52806	5.0	1(.937)	4(.063)		
6	1.9369	1.0	3(1.00)			
7	1.9518	2.0	1(.007)	2(.981)	3(.003)	4(.004)
8	1.9838	3.0	1(.018)	2(.969)	4(.013)	
9	2.2115	1.0-	1(.020)	3(.980)		
10	2.5715	2.0-	1(.760)	2(.213)	3(.016)	9(.011)
11	2.9687	3.0	7(1.00)			
12	3.0596	2.0	2(.150)	7(.850)		
13	3.5192	3.0-	1(.140)	4(.070)	7(.502)	9(.231)
14	3.7066	6.0	4(.680)	5(.320)		
15	3.9435	1.0	3(.930)	7(.070)		
16	4.0713	4.0	5(.130)	8(.870)		
17	4.2961	0.0-	6(.599)	10(.401)		
18	4.319	1.0	3(1.00)			
19	4.36	2.0	1(.182)	2(.060)	7(.758)	
20	4.4683	4.0-	4(.112)	5(.138)	8(.092)	10(.658)
21	4.5238	7.0	5(1.00)			
22	4.5828	2.0-	1(.301)	7(.699)		
23	4.6217	1.0	3(.401)	7(.599)		
24	4.71	5.0	8(.519)	11(.050)	16(.431)	
25	4.771	3.0	7(1.00)			
26	5.0624	2.0	7(1.00)			
27	5.1006	4.0	1(.181)	4(.151)	5(.118)	12(.181)
28	5.131	1.0	7(1.00)			
29	5.174	2.0	2(.833)	8(.167)		
30	5.318	1.0	7(1.00)			
31	5.442	2.0-	1(.387)	2(.613)		
32	5.603	1.0	7(1.00)			
33	5.7	2.0	7(1.00)			

**Table 5 Energy levels and gamma-ray branching ratios (normalized on unity) of  $^{23}\text{Ne}$** 

Levels			Decays		
No.	$E_{lev}(\text{MeV})$	$J^\pi$	Number of state (branching ratio)		
1	0	2.5			
2	1.017	0.5	1(1.00)		
3	1.70151	3.5	1(.980)	2(.020)	
4	1.8225	1.5	1(.980)	2(.020)	
5	2.3151	2.5	1(.471)	2(.080)	3(.030) 4(.419)
6	2.517	3.5	1(.200)	3(.800)	
7	3.22066	1.5-	1(.188)	2(.782)	4(.030)
8	3.4318	1.5	1(.589)	2(.289)	4(.082) 5(.040)
9	3.4582	1.5	2(.451)	4(.549)	
10	3.8309	2.5	1(.087)	2(.038)	3(.875)
11	3.8364	-0.5	2(.559)	4(.441)	
12	3.8433	3.5	6(1.00)		
13	3.9882	1.5	1(.581)	5(.419)	
14	4.01	2.5-	1(1.00)		
15	4.27	1.5-	1(.118)	2(.882)	
16	4.436	3.5	3(.379)	6(.621)	

**Table 6 Energy levels and gamma-ray branching ratios (normalized on unity) of  $^{22}\text{Ne}$** 

Levels			Decays	
No.	$E_{lev}(\text{MeV})$	$J^\pi$	Number of state (branching ratio)	
1	0	0.0		
2	1.27454	2.0	1(1.00)	
3	3.3572	4.0	2(1.00)	
4	4.4567	2.0	1(.030)	2(.970)
5	5.1475	2.0-	2(.529)	4(.471)
6	5.3262	1.0	1(.671)	2(.329)
7	5.365	2.0	1(.100)	2(.900)
8	5.5232	4.0	2(.016)	3(.984)
9	5.6413	3.0	2(.709)	3(.291)
10	5.9099	3.0-	2(.840)	3(.059) 4(.101)
11	6.115	2.0	1(.140)	2(.779) 4(.081)
12	6.237	0.0	2(1.00)	
13	6.3114	6.0	3(1.00)	
14	6.3452	4.0	3(1.00)	
15	6.636	2.0	2(.429)	3(.571)
16	6.691	1.0-	1(.877)	2(.123)
17	6.817	2.0	2(.610)	4(.390)
18	6.8534	1.0	1(.719)	2(.281)
19	6.904	0.0	2(1.00)	
20	7.052	1.0-	1(.090)	2(.910)
21	7.3411	4.0	3(.733)	8(.047) 10(.220)
22	7.342	0.0	4(.167)	6(.833)
23	7.406	3.0-	2(.571)	5(.429)
24	7.423	5.0	8(1.00)	
25	7.47	0.0	2(1.00)	
26	7.489	1.0-	1(.568)	2(.222) 7(.210)
27	7.644	2.0	2(.229)	3(.771)
28	7.664	2.0-	1(.131)	2(.730) 4(.139)
29	7.721	3.0-	2(.151)	3(.229) 4(.521) 11(.099)
30	7.924	2.0	2(1.00)	

**Table 7 Energy levels and gamma-ray branching ratios (normalized on unity) of  $^{21}\text{Ne}$** 

No.	Levels		Decays				
	E <sub>lev</sub> (MeV)	J $\pi$	Number of state (branching ratio)				
1	0	1.5					
2	0.350728	2.5	1(1.00)				
3	1.745909	3.5	1(.050)	2(.950)			
4	2.78883	0.5-	1(.168)	2(.832)			
5	2.79414	0.5	1(.971)	2(.029)			
6	2.8668	4.5	2(.379)	3(.621)			
7	3.66367	1.5-	1(.019)	2(.535)	3(.019)	4(.349)	5(.059)
8	3.7353	2.5	1(.764)	2(.113)	3(.066)	4(.019)	5(.019)
9	3.8843	2.5-	1(.266)	2(.635)	3(.019)	4(.004)	5(.019)
				7(.038)			
10	4.4336	5.5	1(.019)	2(.019)	3(.222)	6(.740)	
11	4.5254	2.5	1(.208)	2(.697)	3(.038)	4(.019)	5(.019)
12	4.6845	1.5	1(.339)	2(.573)	5(.011)	4(.009)	5(.022)
13	4.72536	1.5-	1(.010)	2(.797)	3(.010)	4(.010)	5(.163)
14	5.3357	3.5-	1(.018)	2(.773)	3(.045)	4(.018)	5(.018)
				9(.035)			
15	5.4308	3.5	1(.046)	2(.660)	3(.172)	4(.018)	5(.018)
16	5.549	1.5	1(.294)	2(.091)	4(.121)	5(.141)	8(.232)
17	5.629	3.5	1(.058)	2(.642)	3(.128)	6(.037)	8(.090)
18	5.68977	0.5	1(.386)	2(.019)	4(.019)	5(.502)	6(.019)
19	5.7747	2.5	1(.771)	2(.139)	3(.018)	4(.018)	5(.018)
				8(.018)			
20	5.819	3.5-	1(.038)	2(.161)	3(.049)	4(.019)	6(.228)
				8(.116)	9(.304)	11(.049)	7(.036)
21	5.822	1.5	1(.045)	2(.469)	3(.018)	4(.018)	5(.432)
22	5.99256	1.5-	1(.571)	2(.309)	3(.017)	4(.017)	5(.017)
				8(.026)	9(.017)		6(.026)
23	6.0329	4.5-	1(.027)	2(.027)	3(.410)	4(.018)	5(.018)
				8(.018)	9(.124)	14(.016)	6(.342)
24	6.1738	2.5	1(.045)	2(.329)	3(.412)	4(.047)	8(.148)
25	6.2674	4.5	1(.044)	2(.133)	3(.047)	4(.017)	5(.017)
				8(.027)	9(.017)	10(.033)	6(.665)
26	6.4476	5.5	6(.200)	10(.800)			
27	6.5517	4.5-	1(.071)	2(.024)	3(.511)	4(.024)	5(.032)
				8(.032)	9(.032)	10(.085)	6(.189)
28	6.6081	1.5	1(.041)	2(.821)	3(.027)	4(.017)	5(.017)
				8(.017)	9(.017)		6(.043)
29	6.64	4.5	3(.289)	6(.451)	10(.150)	17(.110)	

**Table 8 Energy levels and gamma-ray branching ratios (normalized on unity) of  $^{20}\text{F}$**

No.	Levels		Decays				
	$E_{lev}(\text{MeV})$	$J^\pi$	Number of state (branching ratio)				
1	0	2.0					
2	0.65602	3.0	1(1.00)				
3	0.82273	4.0	1(.332)	2(.668)			
4	0.98359	1.0-	1(1.00)				
5	1.05685	1.0	1(1.00)				
6	1.30919	2.0-	1(.917)	2(.024)	4(.049)	5(.010)	
7	1.8238	5.0	3(1.00)				
8	1.8438	2.0-	1(.914)	2(.067)	6(.019)		
9	1.97083	3.0-	1(.177)	3(.518)	4(.008)	6(.297)	
10	2.04398	2.0	1(.075)	2(.918)	6(.007)		
11	2.1943	3.0	1(.470)	3(.512)	6(.018)		
12	2.86486	3.0-	1(.380)	2(.050)	3(.120)	6(.120)	8(.070)
			10(.120)	11(.070)			9(.070)
13	2.96611	3.0	1(.271)	2(.122)	3(.583)	11(.024)	
14	2.968	4.0-	3(.390)	9(.610)			
15	3.17169	1.0	4(1.00)				
16	3.48841	1.0	1(.725)	4(.038)	5(.071)	6(.092)	8(.074)
17	3.52631	0.0	5(1.00)				
18	3.58654	2.0	1(.329)	2(.098)	4(.040)	5(.102)	8(.007)
			11(.088)	13(.025)			10(.311)
19	3.5898	3.0-	1(.832)	2(.107)	10(.061)		
20	3.669	1.0	1(1.00)				
21	3.678	1.0-	1(1.00)				
22	3.68017	2.0	1(.465)	2(.171)	5(.235)	6(.043)	8(.086)
23	3.761	3.0	1(.271)	2(.122)	3(.583)	11(.024)	
24	3.96507	1.0	4(.263)	6(.586)	8(.101)	15(.050)	
25	4.08217	1.0	1(.355)	4(.046)	5(.500)	10(.099)	

**Table 9 Energy levels and gamma-ray branching ratios (normalized on unity) of  $^{19}\text{F}$** 

No.	Levels		Decays			
	$E_{lev}(\text{MeV})$	$J^\pi$	Number of state (branching ratio)			
1	0	0.5				
2	0.109894	0.5-	1(1.00)			
3	0.197143	2.5	1(.999)	2(.001)		
4	1.34567	2.5-	2(.968)	3(.032)		
5	1.4587	1.5-	1(.205)	2(.687)	3(.106)	4(.002)
6	1.554038	1.5-	1(.025)	2(.048)	3(.925)	5(.002)
7	2.779849	4.5	3(1.00)			
8	3.90817	1.5	1(.480)	2(.170)	3(.140)	6(.210)
9	3.9987	3.5-	3(.180)	4(.700)	5(.120)	
10	4.0325	4.5-	4(1.00)			
11	4.3777	3.5	1(.047)	2(.019)	3(.752)	7(.182)
12	4.5499	2.5	3(.690)	4(.050)	5(.080)	6(.180)
13	4.5561	1.5-	1(.346)	2(.433)	3(.087)	4(.038)
14	4.648	6.5	7(1.00)			
15	4.6825	2.5-	3(.056)	4(.631)	5(.313)	
16	5.1066	2.5	1(.784)	4(.016)	5(.102)	6(.018)
			11(.020)			
17	5.337	0.5	1(.374)	2(.424)	5(.202)	
18	5.418	3.5-	4(.707)	5(.131)	9(.101)	10(.061)
19	5.4635	3.5	2(.040)	4(.320)	6(.050)	7(.590)
20	5.5007	1.5	2(.248)	3(.485)	4(.158)	6(.109)
21	5.535	2.5	1(.071)	3(.474)	5(.455)	
22	5.621	2.5-	3(.390)	4(.610)		
23	5.938	0.5	1(.069)	2(.195)	3(.020)	5(.618)
24	6.07	3.5	3(.535)	4(.187)	6(.010)	7(.228)
25	6.088	1.5-	1(.250)	2(.610)	3(.140)	11(.040)
26	6.1	4.5-	4(1.00)			
27	6.1606	3.5-	3(.306)	4(.642)	5(.013)	9(.016)
28	6.255	0.5	1(.069)	2(.195)	3(.020)	5(.618)
29	6.282	2.5	1(.140)	3(.042)	4(.359)	5(.259)
30	6.33	3.5	3(.563)	4(.171)	6(.085)	11(.181)
31	6.429	0.5-	1(.250)	2(.140)	8(.610)	
32	6.4967	1.5	1(.380)	2(.140)	3(.090)	4(.140)
33	6.5	5.5	7(.550)	14(.450)		
34	6.5275	1.5	1(.290)	2(.590)	12(.120)	
35	6.554	3.5	3(.190)	4(.550)	7(.260)	
36	6.592	4.5	3(.130)	7(.630)	11(.240)	
37	6.787	1.5-	1(.150)	2(.391)	3(.130)	4(.053)
38	6.8384	2.5	1(.090)	2(.090)	3(.270)	4(.100)
39	6.891	1.5-	1(.090)	4(.610)	5(.300)	
40	6.9265	3.5-	3(.730)	4(.220)	7(.024)	9(.013)
41	6.989	0.5-	1(.300)	2(.190)	8(.510)	
42	7.114	3.5	3(.190)	4(.550)	7(.260)	
43	7.1662	5.5-	9(.056)	10(.909)	14(.035)	
44	7.262	1.5	1(.290)	2(.590)	12(.120)	
45	7.364	0.5	1(.069)	2(.195)	3(.020)	5(.618)
46	7.5396	2.5	3(.290)	4(.012)	6(.411)	11(.270)
47	7.56	3.5	3(.210)	4(.570)	7(.220)	
48	7.587	2.5-	3(.056)	4(.631)	5(.313)	
49	7.6606	1.5	1(.376)	3(.129)	6(.357)	8(.030)
					12(.050)	16(.058)

**Table 10 Level density parameters**

Residual nuclei	T (MeV)	$E_0$ (MeV)	a ( $\text{MeV}^{-1}$ )	$\Delta$ (MeV)	$\sigma$	$E_m$ (MeV)
$^{24}\text{Na}$	1.7136	-1.4621	4.09	0	4.061	7.00
$^{23}\text{Na}$	2.3500	-1.1700	3.35	2.29	5.024	12.00
$^{22}\text{Na}$	2.2769	-2.2903	3.17	0	6.000	10.00
$^{23}\text{Ne}$	1.8643	-0.6166	4.30	2.29	3.202	10.25
$^{22}\text{Ne}$	1.8110	1.7324	4.47	4.69	4.772	13.40
$^{21}\text{Ne}$	2.2046	-0.7293	3.52	2.40	5.612	11.45
$^{20}\text{F}$	1.9300	-1.9116	3.71	0	3.774	8.00
$^{19}\text{F}$	2.7362	-2.7724	3.09	2.52	5.277	15.3

T =nuclear temperature

 $E_0$  =normalization parameter

a =Fermi-gas level density parameter

 $\Delta$  =pairing energy $\sigma$  =spin cutoff parameter $E_m$  =energy at the boundary between the temperature and Fermi-gas level density region

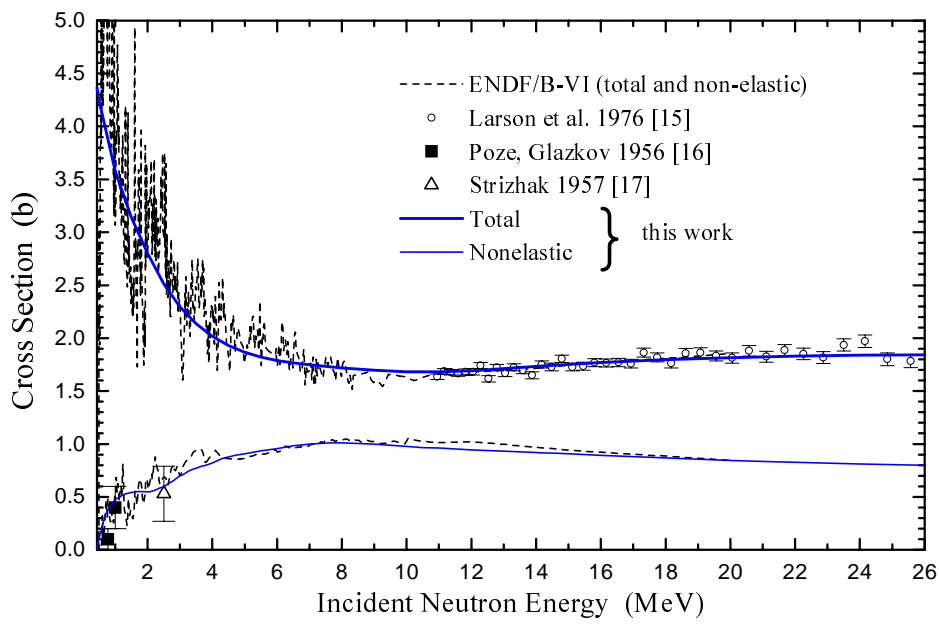


Fig.1. Total and nonelastic cross sections for neutrons on  $^{23}\text{Na}$ .

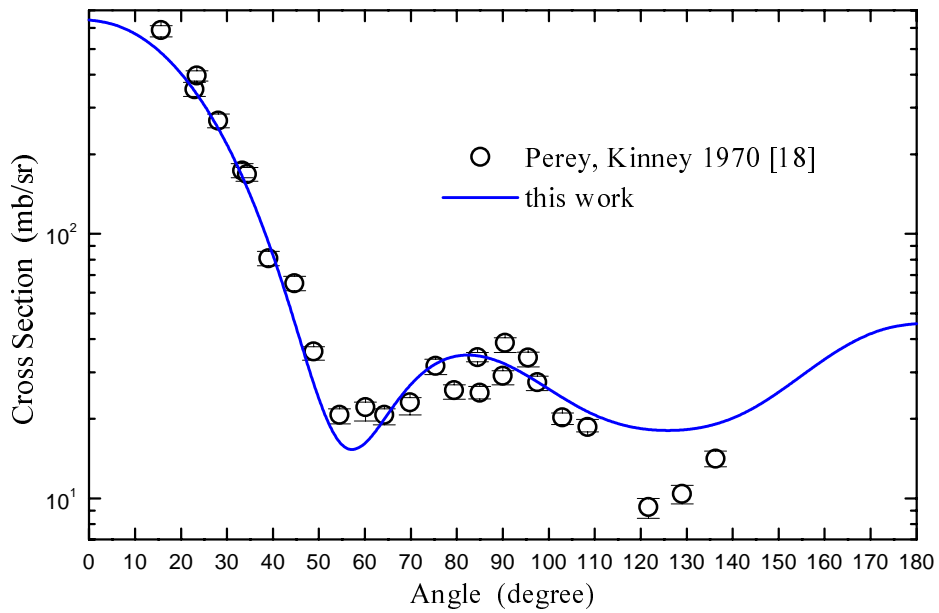


Fig. 2. Differential elastic cross section of  $^{23}\text{Na}$  at 7.6 MeV incident neutron energy.

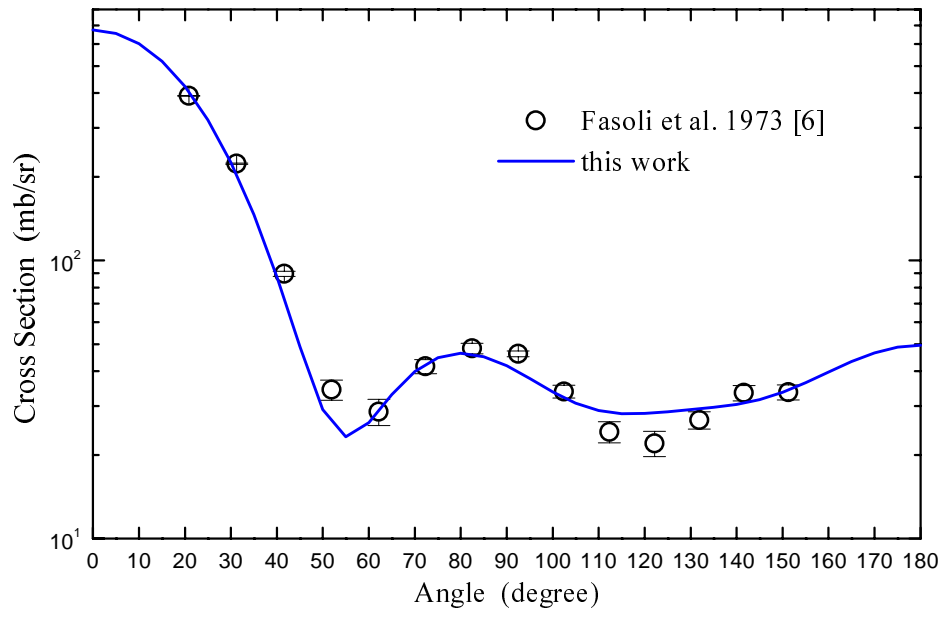


Fig. 3. Sum of differential elastic cross section and inelastic cross section to the 0.44 MeV level of  $^{23}\text{Na}$  at 8.0 MeV incident neutron energy.

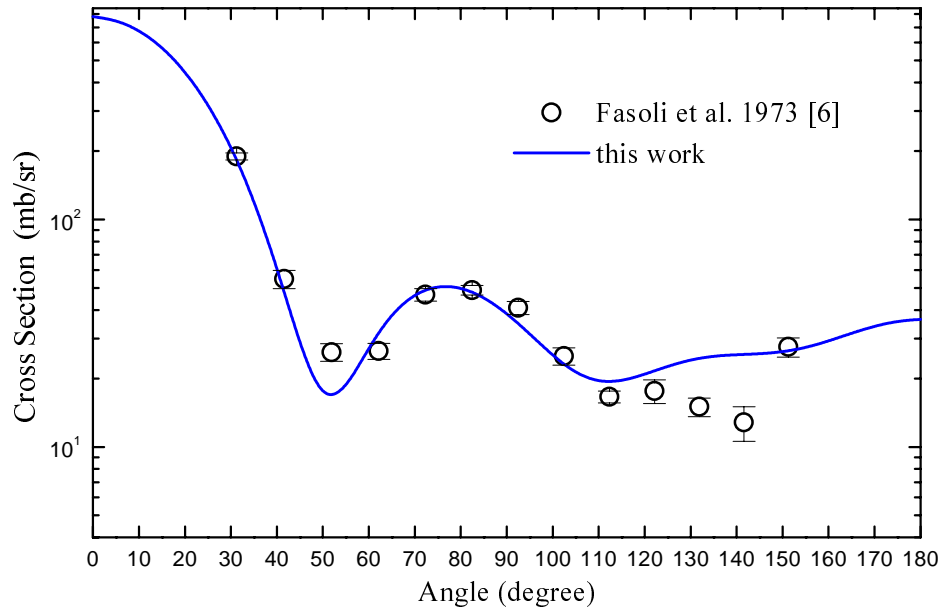


Fig. 4. Sum of differential elastic cross section and inelastic cross section to the 0.44 MeV level of  $^{23}\text{Na}$  at 9.7 MeV incident neutron energy.

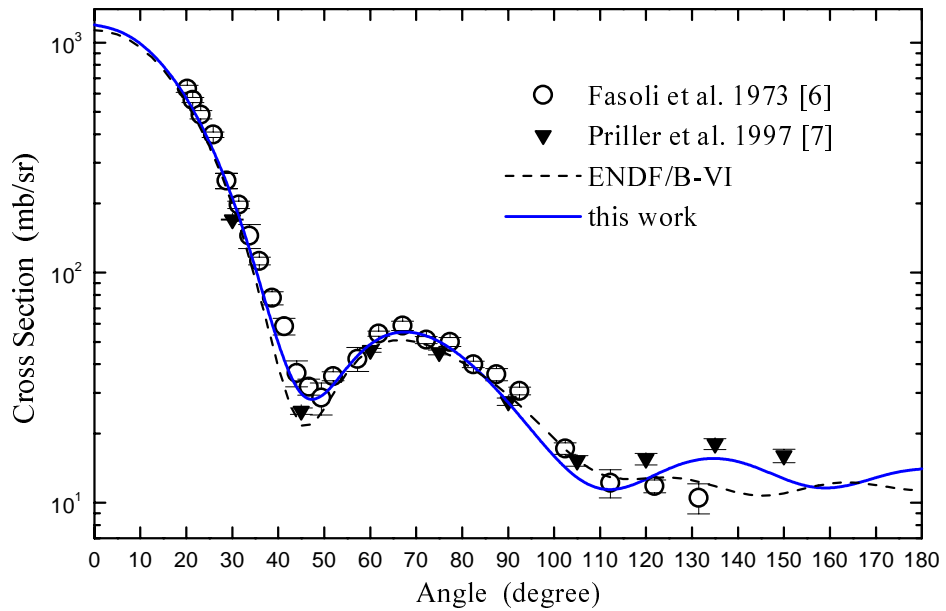


Fig. 5. Sum of differential elastic cross section and inelastic cross section to the 0.44 MeV level of  $^{23}\text{Na}$  at 14.1 MeV incident neutron energy.

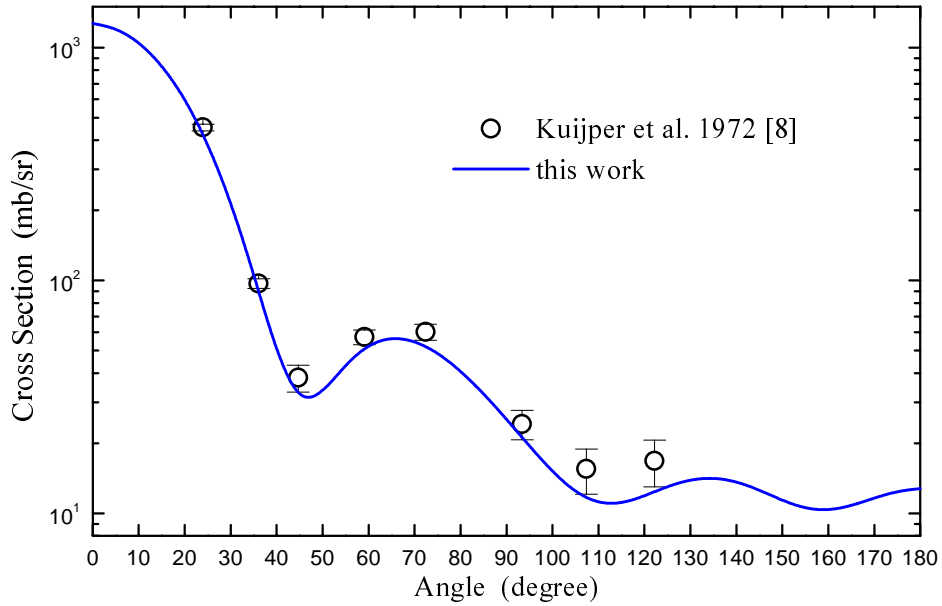


Fig. 6. Sum of differential elastic cross section and inelastic cross section to the 0.44 MeV level of  $^{23}\text{Na}$  at 14.76 MeV incident neutron energy.

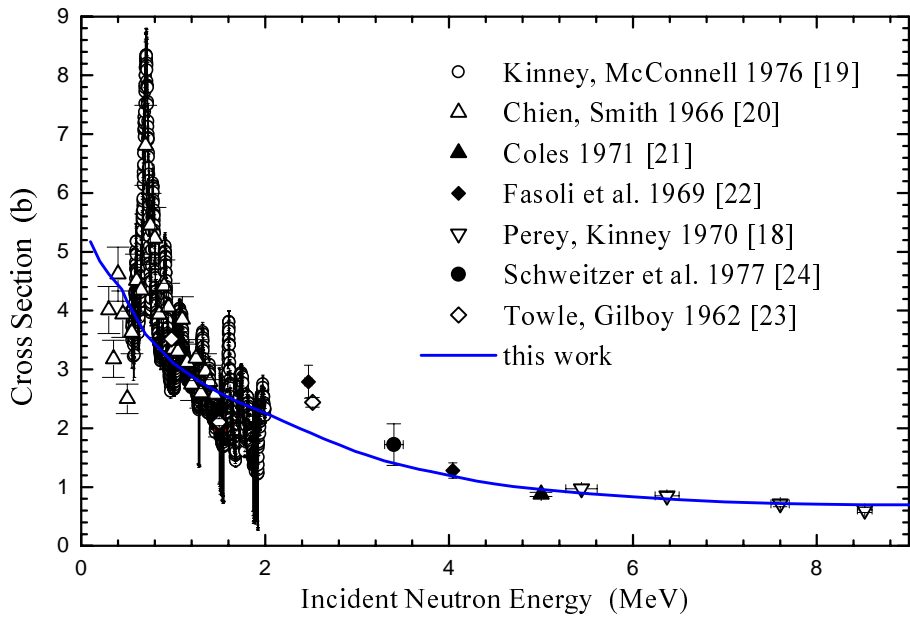


Fig.7. Elastic scattering cross section for neutrons on  $^{23}\text{Na}$ .

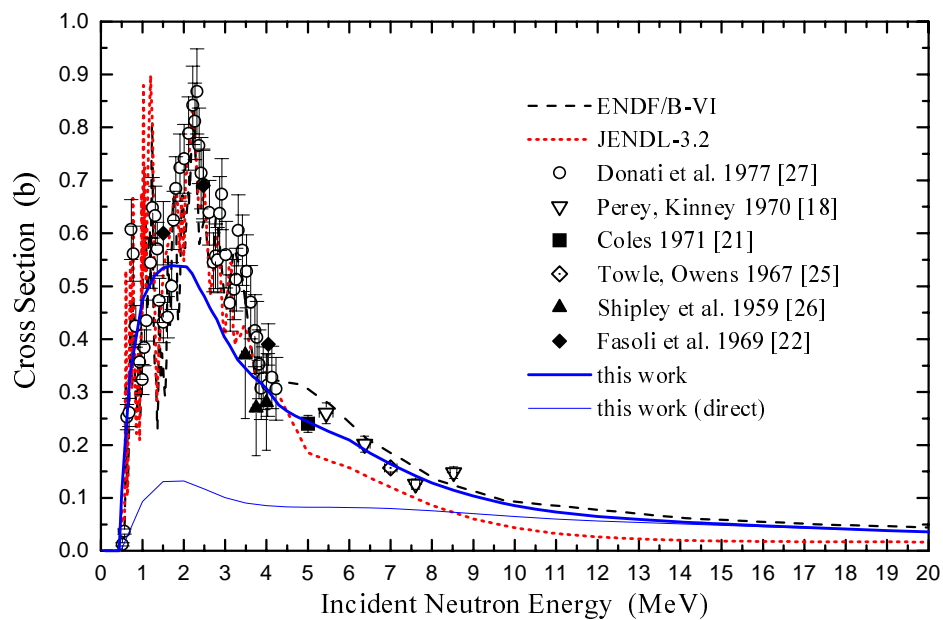


Fig.8.  $^{23}\text{Na}(n,n')$  cross section for exciting 0.439 MeV level.

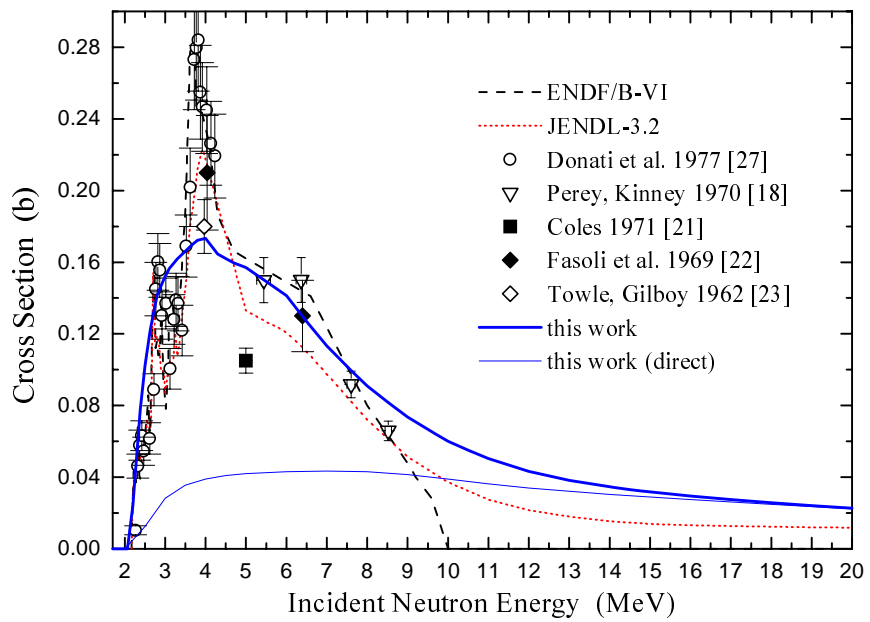


Fig.9.  $^{23}\text{Na}(\text{n},\text{n}'')$  cross section for exciting 2.076 MeV level.

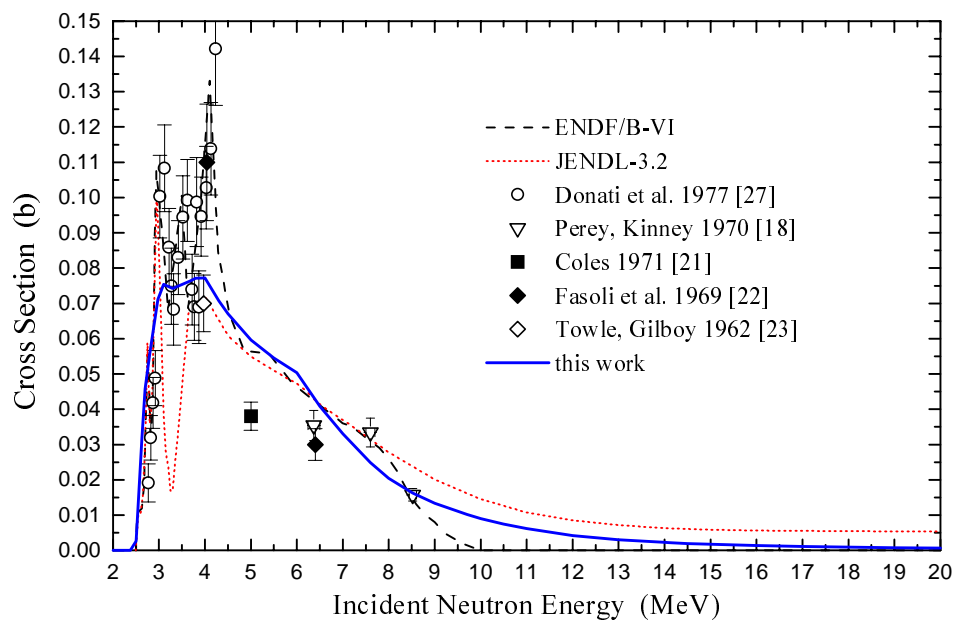


Fig.10.  $^{23}\text{Na}(\text{n},\text{n}'')$  cross section for exciting 2.391 MeV level.

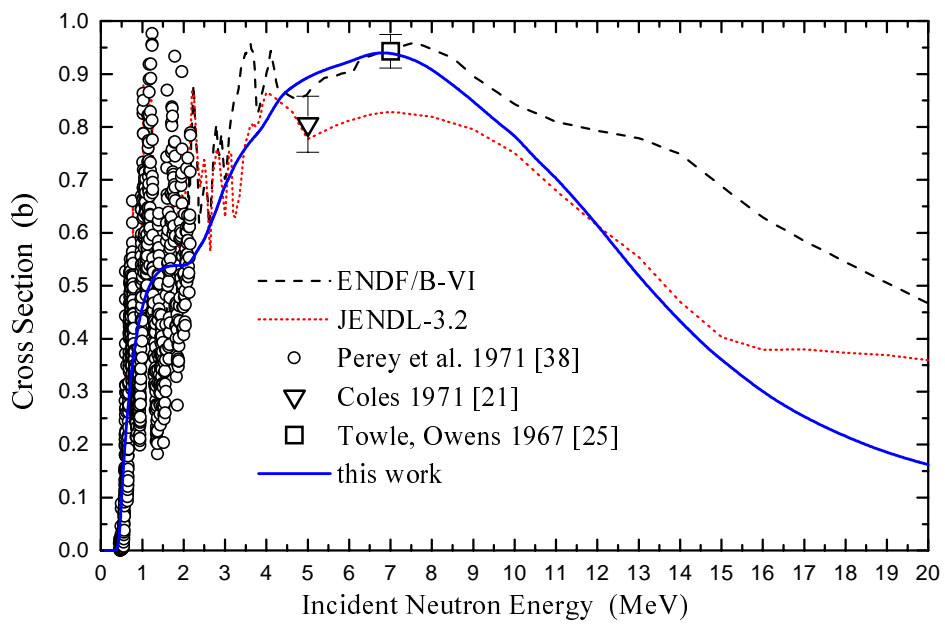


Fig.11.  $(n,n')$  cross section on  $^{23}\text{Na}$ .

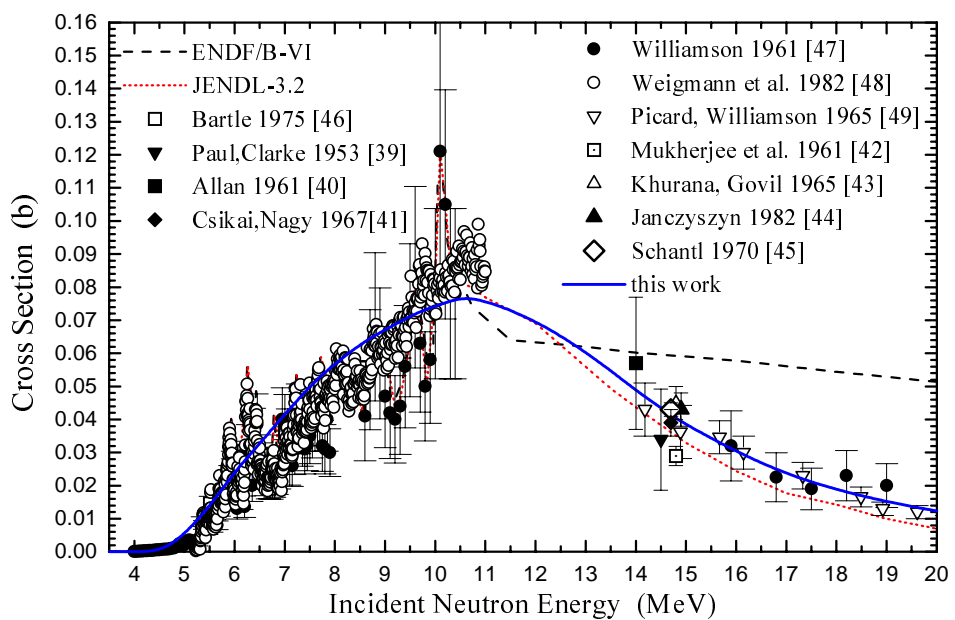


Fig.12.  $(n,p)$  cross section on  $^{23}\text{Na}$ .

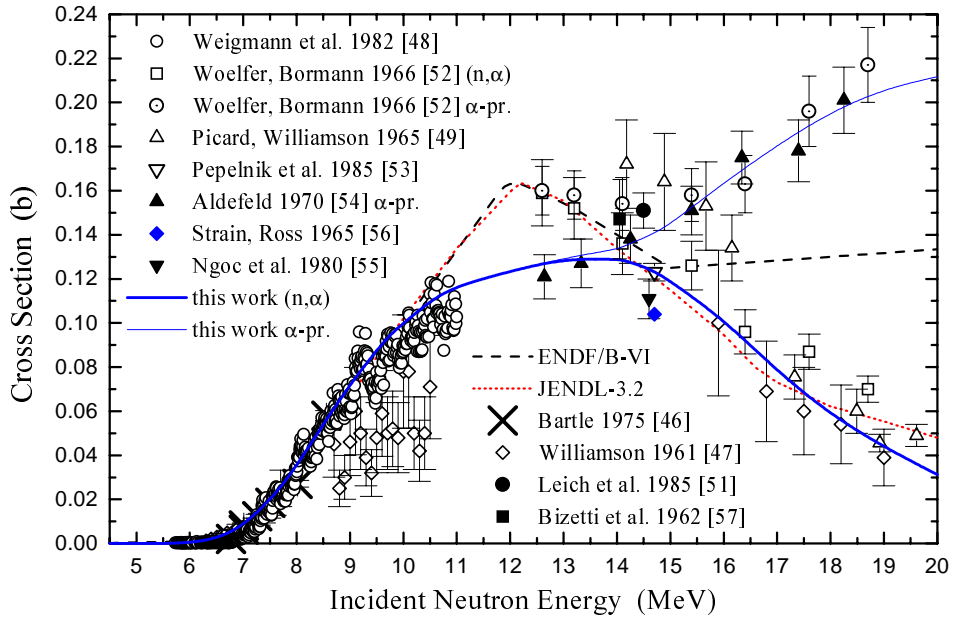


Fig.13.  $(n,\alpha)$  and  $\alpha$ -production cross section on  $^{23}\text{Na}$ .

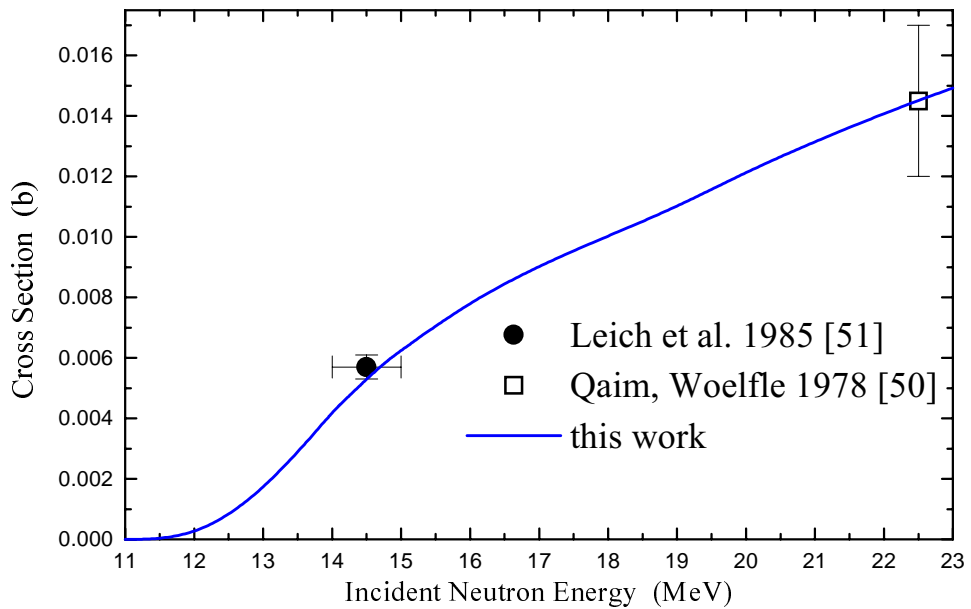


Fig.14.  $(n,t)$  cross section on  $^{23}\text{Na}$ .

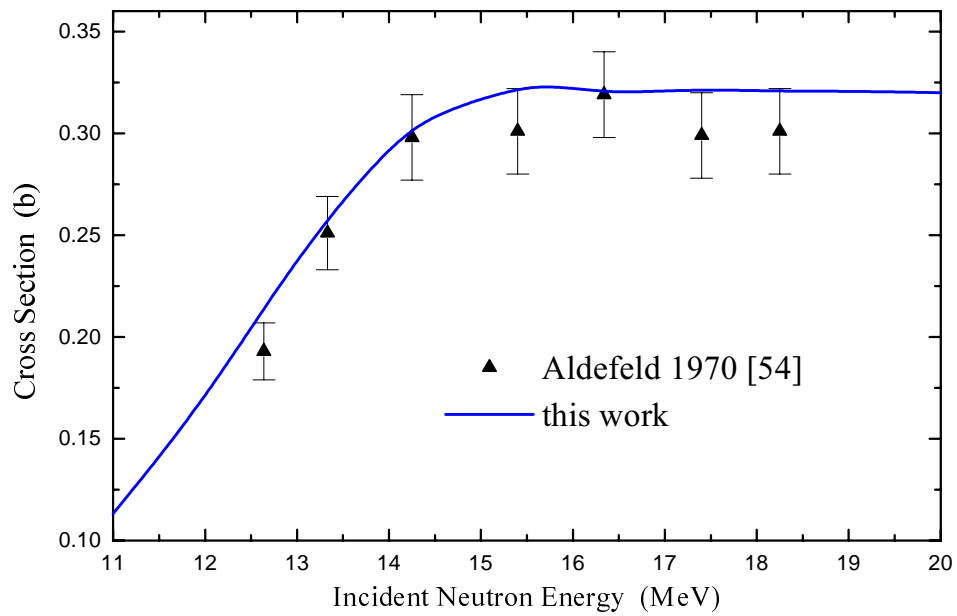


Fig.15. Proton and deuteron production from the reaction system  $^{23}\text{Na} + \text{neutron}$  (outgoing particle energy  $> 1$  MeV).

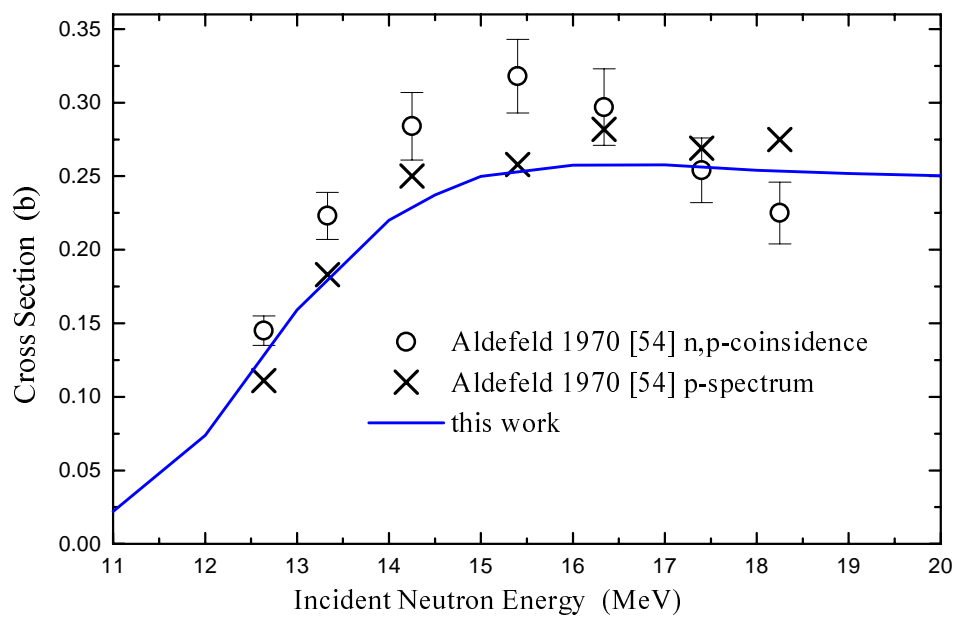


Fig.16. Proton production from the reactions  $^{23}\text{Na}[(\text{n},\text{np})+(\text{n},\text{pn})]$  (proton energy  $> 1$  MeV).

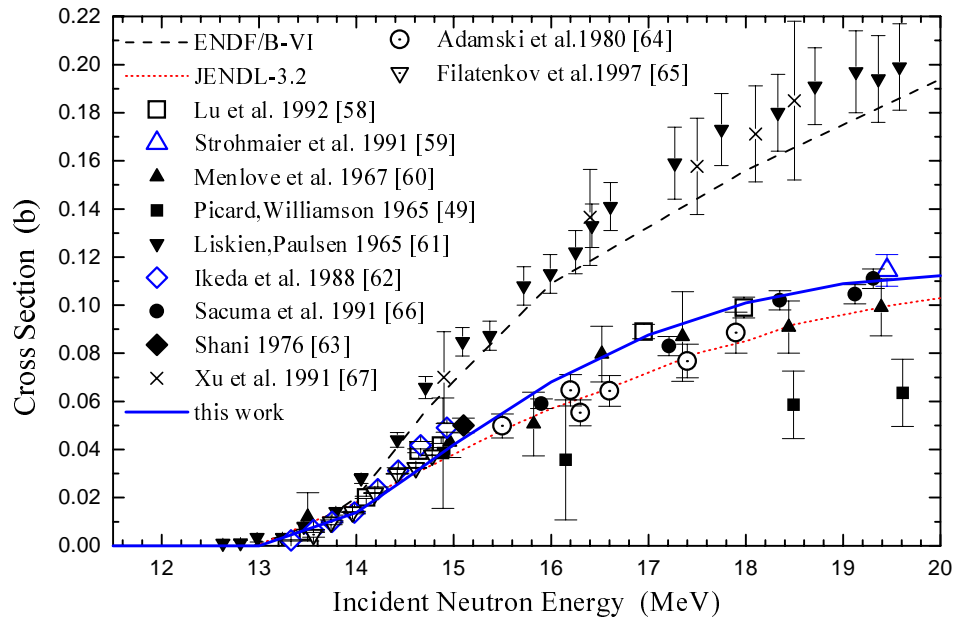


Fig.17.  $(n,2n)$  cross section on  $^{23}\text{Na}$ .

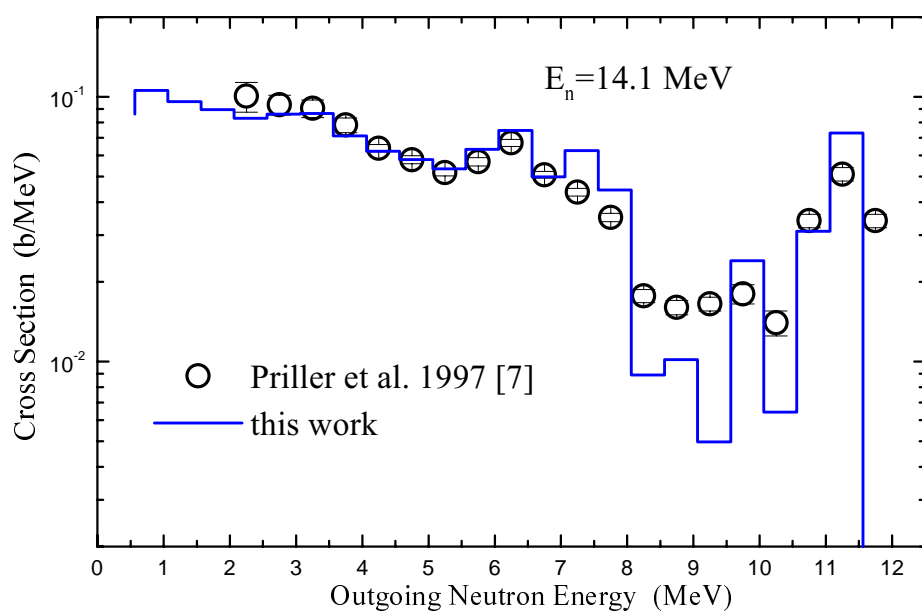


Fig.18. Neutron production spectrum resulting from reactions of 14.1-MeV neutrons with  $^{23}\text{Na}$ .

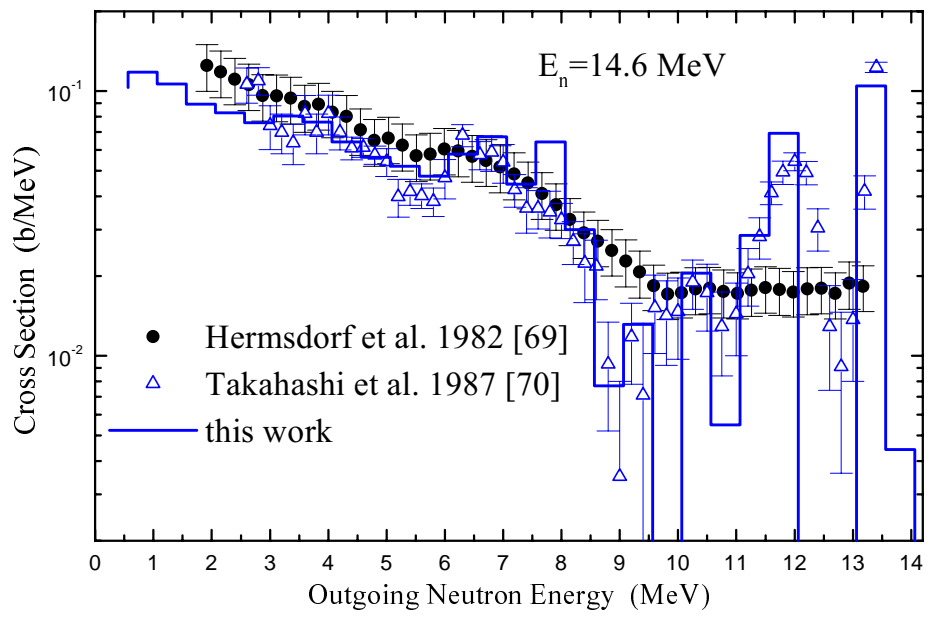


Fig.19. Neutron production spectrum resulting from reactions of 14.6-MeV neutrons with  $^{23}\text{Na}$ .

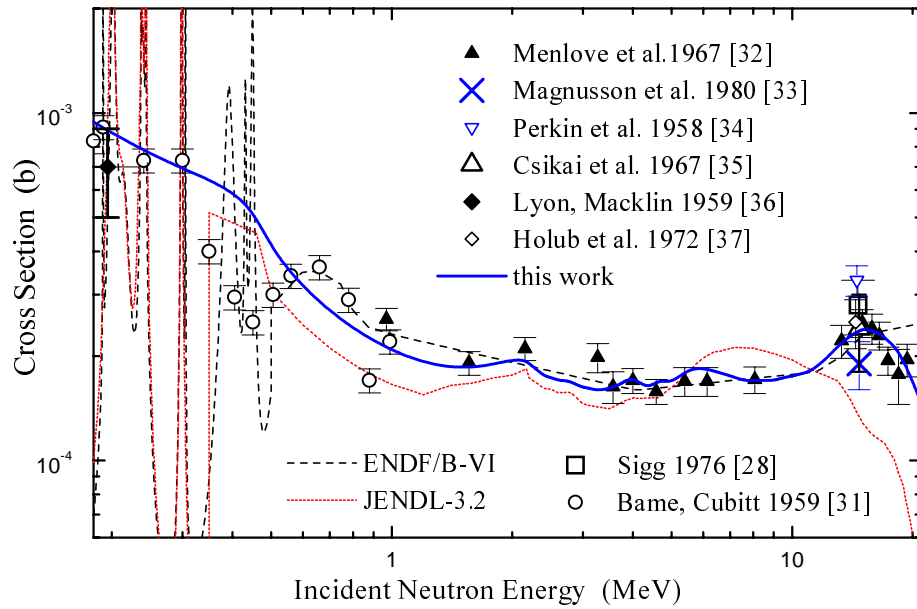


Fig.20. Neutron capture cross section.

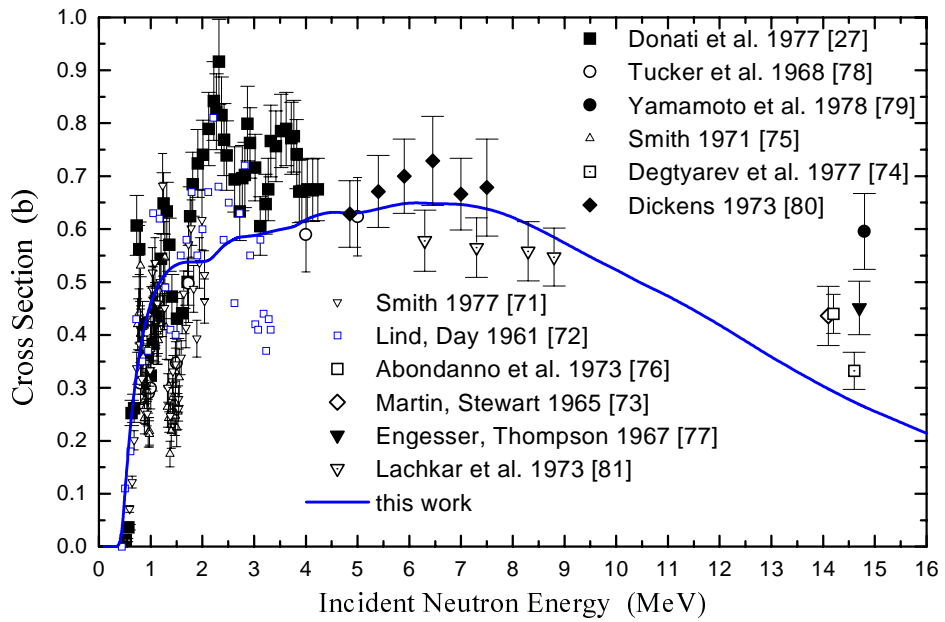


Fig.21. Cross section for the production of the 0.439 MeV gamma ray from the  $^{23}\text{Na}$  ( $n, n'\gamma$ ) reaction.

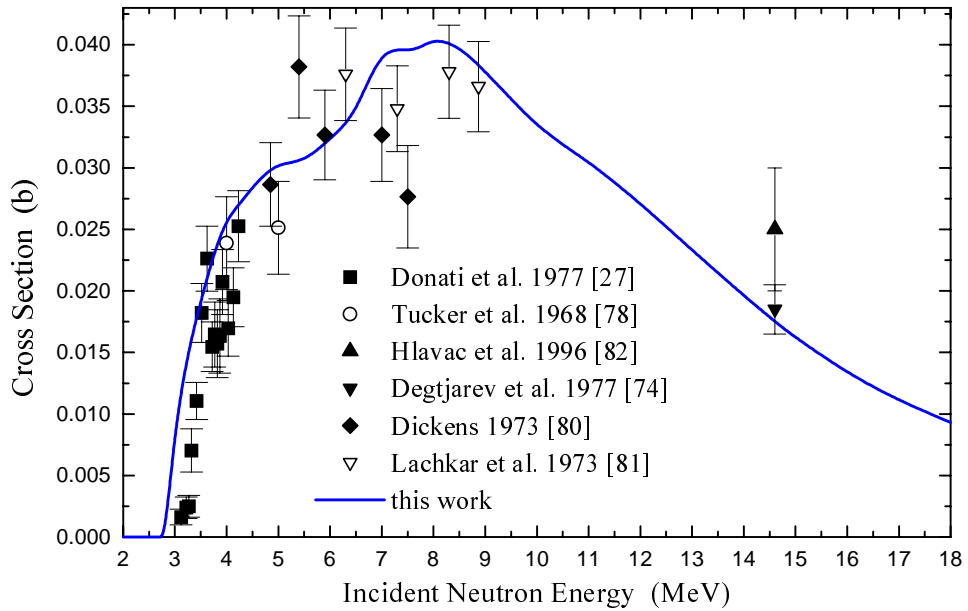


Fig.22. Cross section for the production of the 0.628 MeV gamma ray from the  $^{23}\text{Na}$  ( $n, n'\gamma$ ) reaction.

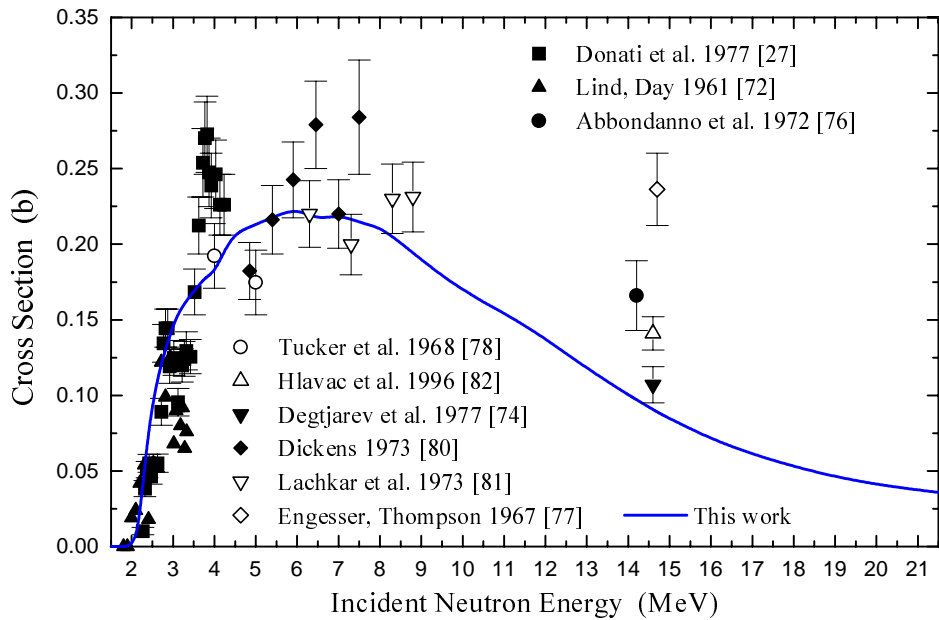


Fig.23. Cross section for the production of the 1.636 MeV gamma ray from the  $^{23}\text{Na}$  ( $n, n'\gamma$ ) reaction.

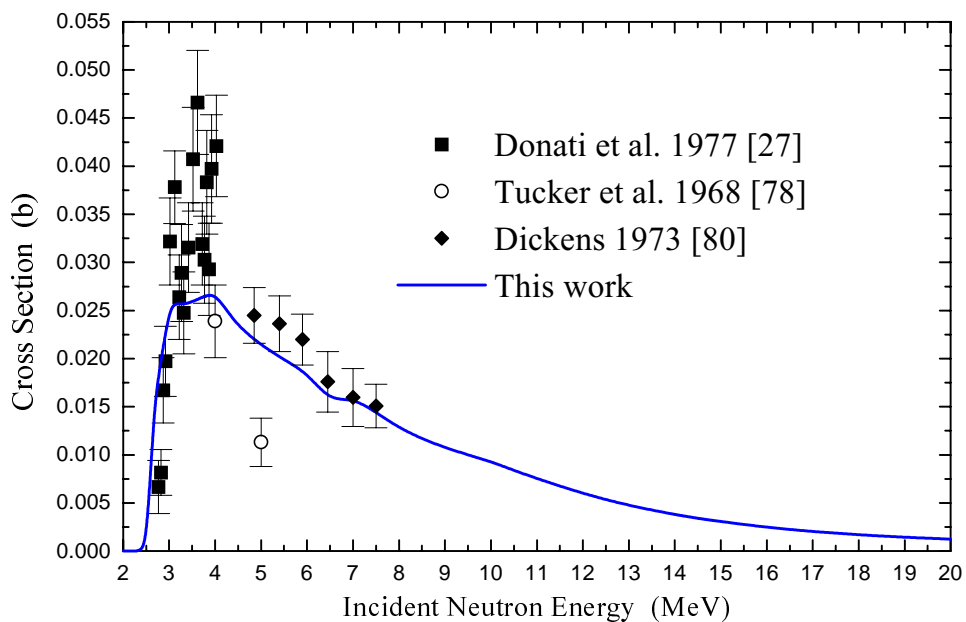


Fig.24. Cross section for the production of the 1.951 MeV gamma ray from the  $^{23}\text{Na}$  ( $n, n'\gamma$ ) reaction.

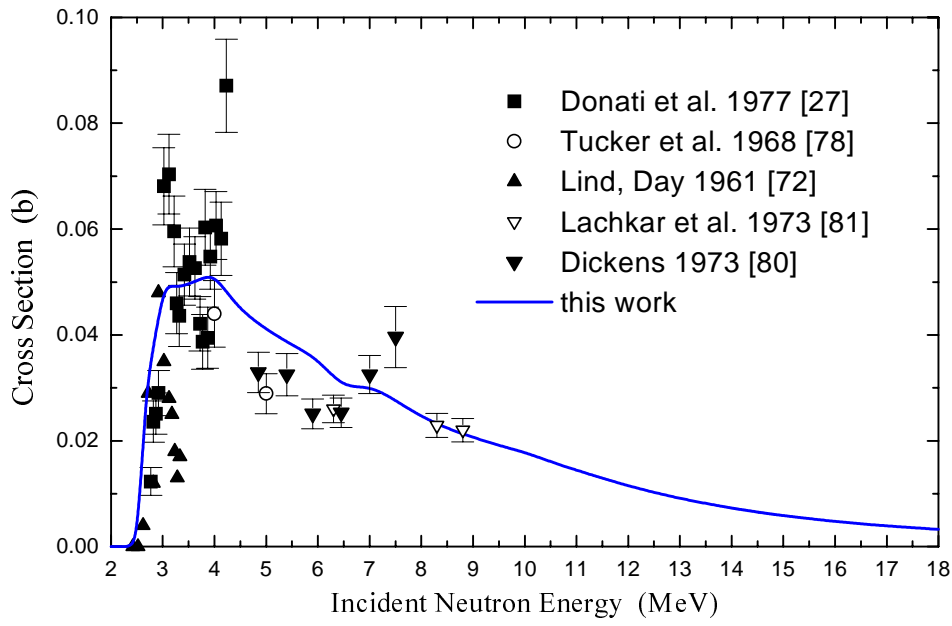


Fig.25. Cross section for the production of the 2.391 MeV gamma ray from the  $^{23}\text{Na}$  ( $n, n'\gamma$ ) reaction.

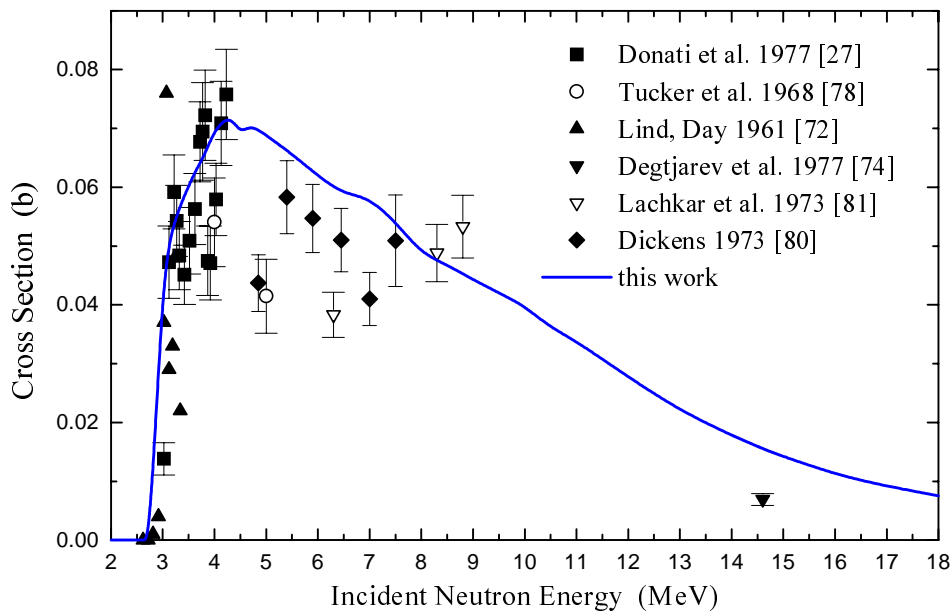


Fig.26. Cross section for the production of the 2.64 MeV gamma ray from the  $^{23}\text{Na}$  ( $n, n'\gamma$ ) reaction.

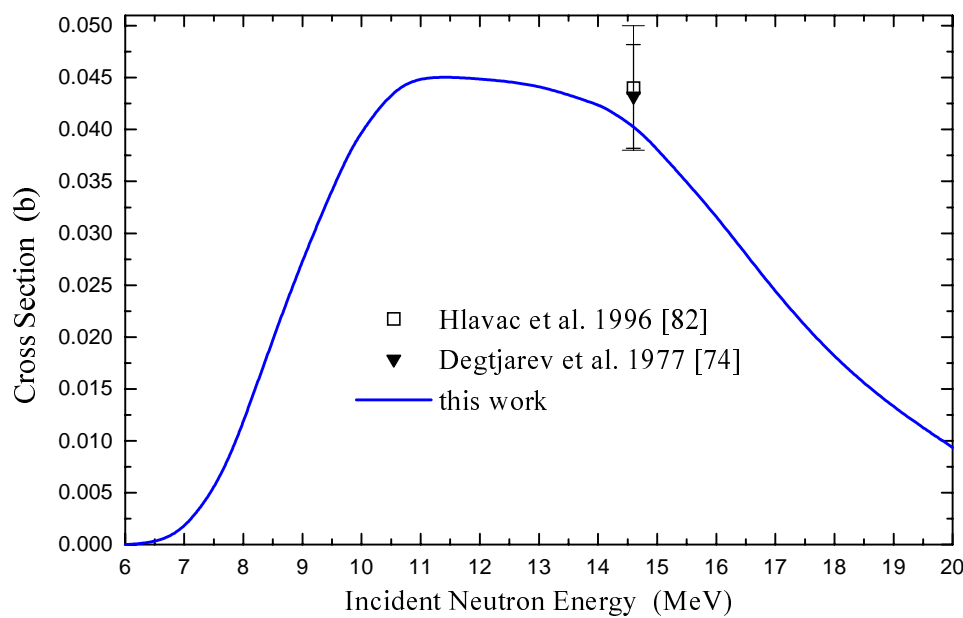


Fig.27. Cross section for the production of the 0.656 MeV gamma ray from the  $^{23}\text{Na}$  ( $n,\alpha\gamma$ ) reaction.

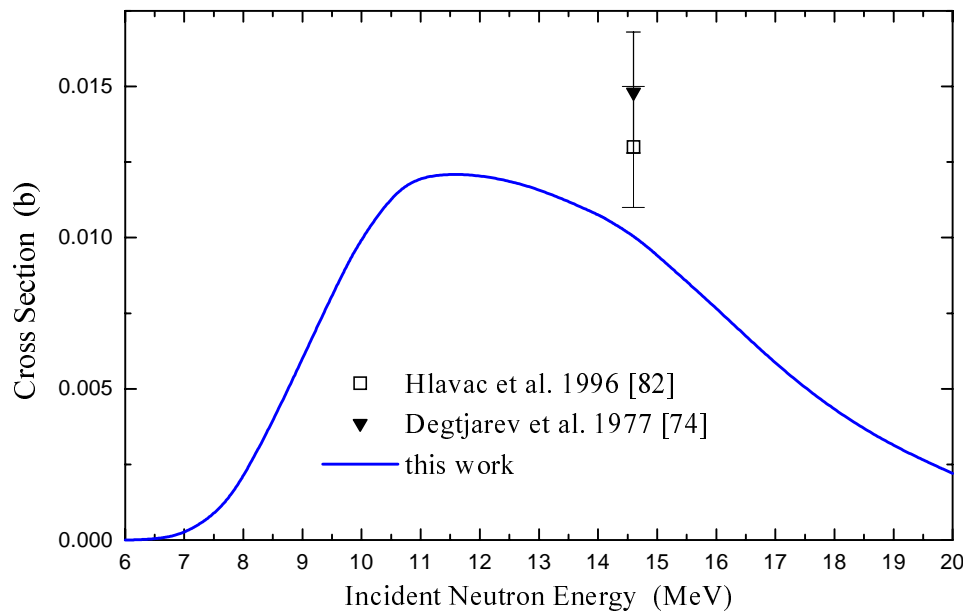


Fig.28. Cross section for the production of the 0.823 MeV gamma ray from the  $^{23}\text{Na}$  ( $n,\alpha\gamma$ ) reaction.

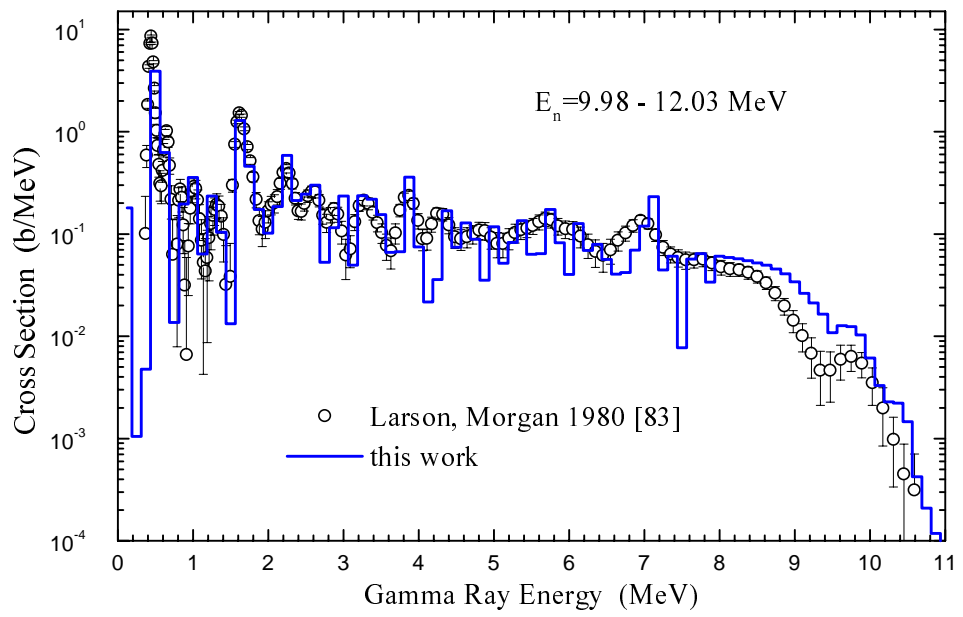


Fig.29. Secondary gamma-ray spectra at average incident neutron energy  $E_n=11.005 \text{ MeV}$ .

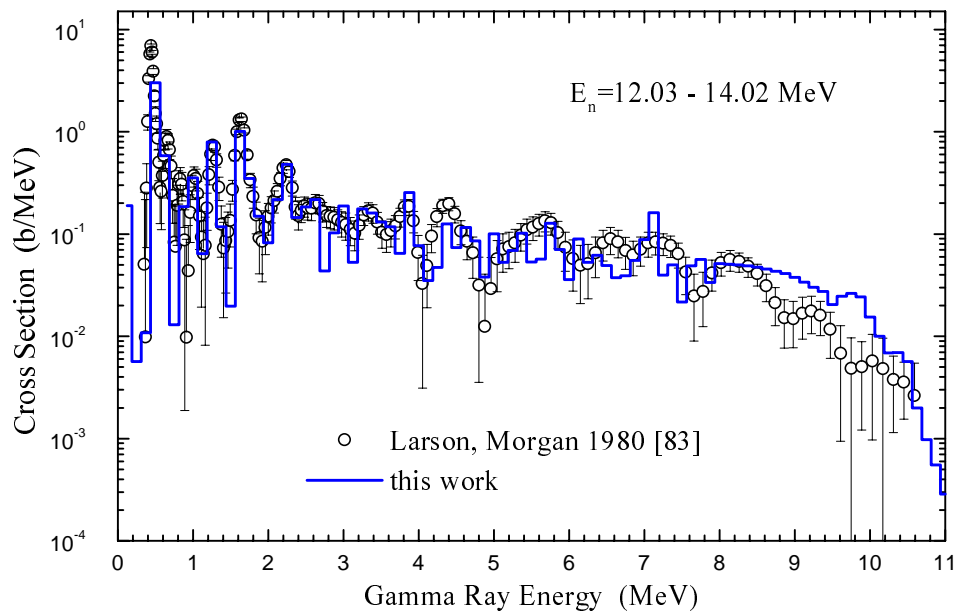


Fig.30. Secondary gamma-ray spectra at average incident neutron energy  $E_n=13.025 \text{ MeV}$ .

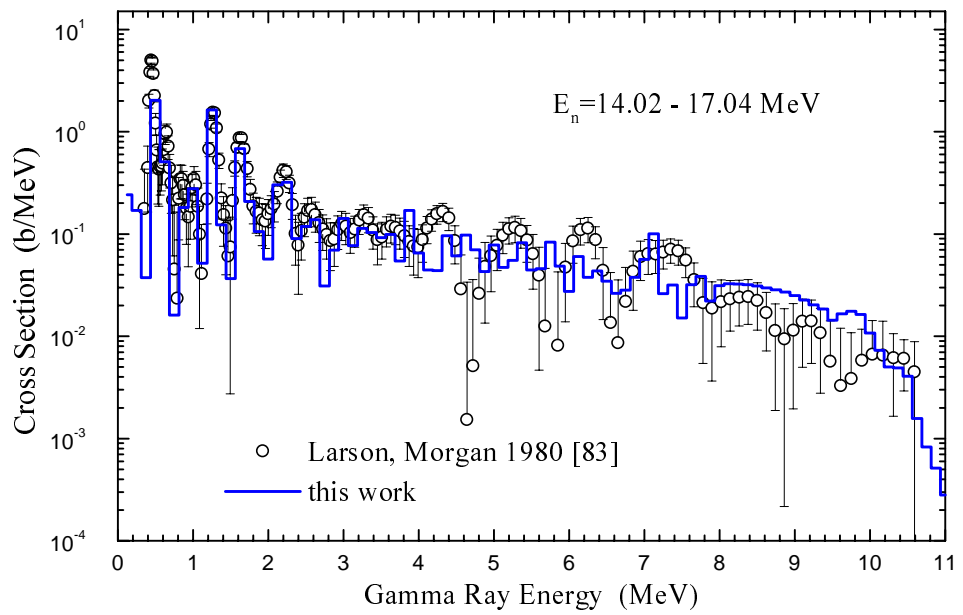


Fig.31. Secondary gamma-ray spectra at average incident neutron energy  $E_n=15.53$  MeV.

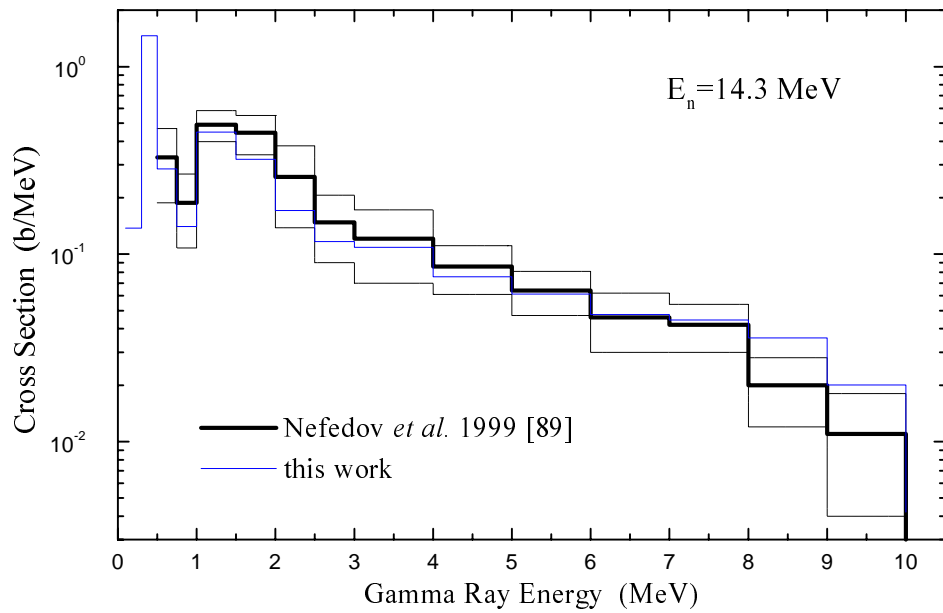


Fig.32. Secondary gamma-ray spectra at the incident neutron energy  $E_n=14.3$  MeV.

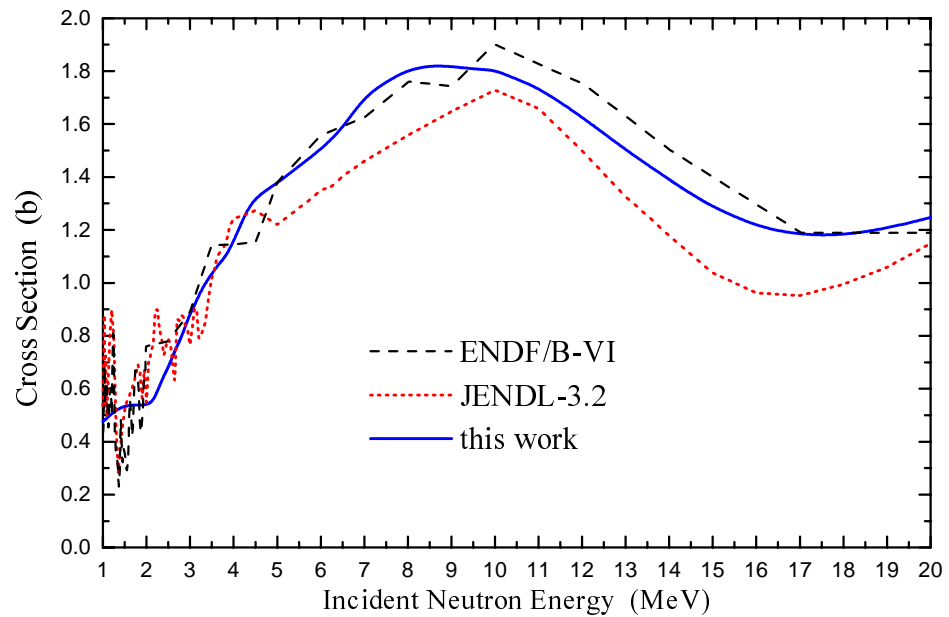


Fig.33. Gamma-production cross section for neutrons on  $^{23}\text{Na}$ .

---

Nuclear Data Section  
International Atomic Energy Agency  
P.O. Box 100  
A-1400 Vienna  
Austria

e-mail: services@iaeand.iaea.or.at  
fax: (43-1) 26007  
cable: INATOM VIENNA  
telex: 1-12645  
telephone: (43-1) 2600-21710

---

Online: TELNET or FTP: iaeand.iaea.or.at  
username: IAEANDS for interactive Nuclear Data Information System  
usernames: ANONYMOUS for FTP file transfer;  
FENDL2 for FTP file transfer of FENDL-2.0;  
RIPL for FTP file transfer of RIPL;  
NDSOOL for FTP access to files sent to NDIS "open" area.

---

Web: <http://www-nds.iaea.or.at>